POLITECNICO
MILANO 1863

SCUOLA DI INGEGNERIA INDUSTRIALE
E DELL'INFORMAZIONE

A review of modeling of Variable Stiffness laminates

Tesi di Laurea Magistrale in
Aeronautical Engineering - Ingegneria Aeronautica

Author: **Rachele Magno**

Student ID: 249006
Advisor: Prof. Riccardo Vescovini
Co-advisors:
Academic Year: 2024-25

Abstract

The present work provides an overview of the state-of-the-art regarding the behavior of variable stiffness composite laminates by progressively moving from classical laminate concepts toward manufacturing compatible descriptions of steered fiber architectures. Conventional laminates with straight and constant fiber orientations are first considered, emphasizing the intrinsic limitations associated with uniform fiber direction within each ply when structures are subjected to spatially varying stress fields and compressive instability phenomena. The transition toward curvilinear and steered fiber configurations is then examined. Physically motivated design strategies based on principal stress directions and global load paths are discussed, highlighting their capability to redistribute stresses and improve tensile, bearing, and buckling performance. Subsequently, computational approaches are analyzed in which fiber orientation is treated as a continuous design variable within a finite element framework. Optimization formulations based on laminate compliance tensors enable systematic stiffness redistribution and demonstrate significant increases in critical buckling load without changes in structural mass. Manufacturing aspects associated with Automated Fiber Placement are addressed, with particular attention to the structural implications of gaps and overlaps generated during tow deposition. Numerical and experimental investigations indicate that resin rich regions associated with gaps reduce in plane stiffness and stability, whereas overlap induced thickness build up enhances bending stiffness and delays buckling.

Robotic Automated Fiber Placement is presented as a manufacturing aware framework in which steering limitations, course discretization, and laminate build up are incorporated directly into the definition of fiber trajectories. Fiber paths are described using cubic Bézier splines controlled through a structured manufacturing mesh, ensuring geometric continuity and compatibility with deposition constraints.

Finally, a geometric modeling framework implemented in MATLAB is introduced to characterize the local laminate architecture associated with prescribed steered fiber paths. By discretizing a perforated panel with triangular elements and determining the number of tows intersecting each nodal location, the model generates a spatial thickness distribution consistent with theoretical geometric expectations, providing a basis for subsequent

structural analyses of stiffness and buckling behavior.

Contents

List of Figures

List of Tables

Introduction

Classical composite laminates represent one of the most used materials in the aeronautical field, thanks to their excellent mechanical performance combined with significant weight savings. The continuous demand for lightweight structures with high strength and high stiffness has led to the extensive use of laminated composite materials in plenty of aircraft components. A classical laminate is formed by stacking multiple thin layers, commonly referred to as laminae or plies, which are bonded together to create a single structure. Each lamina typically consists of a polymeric matrix, most commonly an epoxy resin, reinforced with high performance fibers generally made with carbon or glass. Within an individual lamina, the reinforcing fibers are arranged in a straight, parallel configuration and maintain a constant orientation over the entire surface of the ply. The overall mechanical behavior of a laminate is not solely determined by the properties of the constituent materials but is strongly influenced by the stacking sequence and fiber orientation of the individual plies. By varying the orientation angles of the fibers from one ply to another, it is possible to tailor the global stiffness and strength characteristics of the laminate to meet specific load requirements while maintaining the structure as lightweight as possible. This design flexibility allows optimization of the laminate response under complex loading conditions, such as combined tension, compression, bending, and shear, which are commonly encountered in aeronautical structures. From a mechanical point of view, classical laminates exhibit a fundamentally anisotropic behavior, as their properties differ depending on the direction of loading but this feature, rather than being a limitation, is deliberately exploited in aerospace design to align material stiffness and strength with the principal load paths, thereby improving structural efficiency and reducing unnecessary mass.

The theoretical framework most commonly used to describe the behavior of classical laminates is the Classical Laminate Theory (CLT). This theory is based on a set of simplifying assumptions, including linear elastic behavior of each lamina, perfect bonding between adjacent plies, and constant fiber orientation within each layer. Under these hypothesis, the laminate response can be described through stiffness matrices that relate in-plane forces and bending moments to mid-plane strains and curvatures. Despite its simplifications,

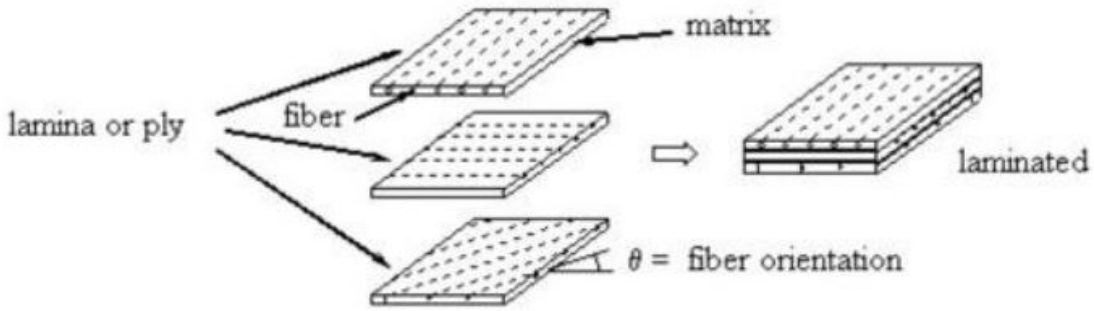

Figure 1: Example of a typical laminate. Source: [16]

CLT has proven to be highly effective and remains a key tool in the analysis and preliminary design of composite aeronautical structures. Although classical laminates have demonstrated excellent performance and reliability over decades of application, their design is inherently constrained by the requirement that fiber orientations remain constant within each ply and, as a result, the load carrying capability of the laminate can only be optimized only through discrete changes in fiber angle between layers. This limitation becomes particularly relevant in structures subjected to spatially varying stress fields where a more continuous adaptation of fiber trajectories could lead to further improvements in structural efficiency. These considerations had conducted the development of innovative composite concepts, such as curvilinear fiber laminates, in which fiber paths are allowed to change their orientation angle in the plane of the ply. Such materials represents an evolution of the classical composites laminates that has the same fundamental principles with enhanced performances under complex loading conditions.

1 | Variable-stiffness laminates and manufacturing aspects

This chapter introduces variable stiffness composite laminates and describes their evolution from physically motivated fiber steering concepts to optimization based and manufacturing aware design approaches. Curvilinear fiber layouts derived from principal stress directions and load paths are first discussed, followed by computational frameworks in which fiber orientation is treated as a continuous design variable to enable stiffness redistribution and improved buckling performance. The chapter concludes with an examination of the structural effects of Automated Fiber Placement induced gaps and overlaps.

1.1. Curvilinear fiber concepts and physically motivated design

The possibility of employing curvilinear fibers was first introduced by Hyer[1], who argued that, although classical composite laminates were already widely established and extensively used in structural applications, their full potential had not yet been completely exploited. He observed that in conventional laminates with straight fibers, the load is carried in an identical manner throughout the laminate, regardless of the local stress state. When such laminates are subjected to complex loading conditions, this uniform load transfer leads to the development of regions characterized by high stress concentrations. Furthermore, in the presence of geometric complexities (such as holes or other structural discontinuities) some fibers must be terminated prematurely. In these regions, the load is consequently transferred to the matrix, which is less efficient in load bearing and was not designed to sustain such stresses.

To overcome these limitations, the author proposed aligning the fibers along the principal load-carrying directions. In order to determine the optimal fiber trajectories, he developed an iterative numerical procedure capable of identifying suitable curvilinear paths. The resulting mathematical model proved to be both computationally efficient and highly

accurate, achieving convergence within a limited number of iterations. This approach enabled the placement of fibers without the need for termination, as the fibers were able to smoothly follow the structural geometry and adapt to variations in the stress field. As a result, load transfer became more efficient, and stress concentrations associated with fiber discontinuities were significantly reduced. To assess the validity of his hypothesis, tensile failure and linear buckling analyses were conducted under compressive loading on different laminate configurations. The objective was to evaluate and compare the maximum load levels sustained in both tension and compression by each laminate type, normalized with respect to the load bearing capacity of a quasi-isotropic laminate. The results obtained from these tests are reported in Table 1.1.

Laminate	Type of material	Load level	Critical load
$(\pm 45/0/90)_2 s$	Quasi-isotropic, straight fibers	1.00	1.00
$(0°)_s$	Unidirectional, straight fibers	0.59	0.46
$(C\theta)_s$	All curvilinear plies	1.01	0.52
$(0/C\theta)_s$	2 orthogonal and 14 curvilinear plies	1.89	0.55
$(\pm 45/C\theta)_s$	Curvilinear and ±45 plies	1.60	0.87
$(\pm 45/0°)_s$	Straight fibers and ±45 plies	1.27	0.84
$(\pm 45/C\theta)_2 s$	Curvilinear and ±45 plies, symmetric	1.33	0.93
$(\pm 45/0°)_2 s$	Straight fibers and ±45 plies, symmetric	1.20	0.90

Table 1.1: Normalized tensile failure loads and critical buckling loads of the laminates. Source: [1]

It is demonstrated that laminates specifically optimized for tension through curvilinear fiber layouts achieve the highest tensile failure loads however, these configurations generally exhibit a reduction in compressive buckling resistance, highlighting the need to consider both loading conditions when assessing overall structural performance. Among the laminates investigated, the configuration that combines curvilinear plies with ±45° layers provides the most favorable compromise between tensile strength and buckling resistance. These laminates present a significant improvement in tensile capacity while maintaining critical buckling loads close to those of conventional quasi-isotropic designs. This observation suggests that fiber steering should not be applied in isolation, but rather integrated within hybrid laminate architectures to ensure balanced mechanical behavior. Building on these numerical findings, subsequent studies have extended the curvilinear fiber concept by exploring alternative design strategies, such as the one published by Tosh and Kelly [3].

The research proposes a different method to design steered laminates: instead of using curvilinear fiber layout based on principal stress directions it recommend the creation of

fibers trajectory based on the load paths. The load paths are regions in which the load in a selected direction remains constants through all the structure.

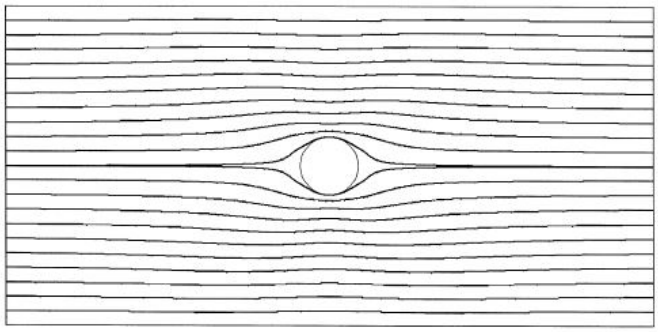

Figure 1.1: X-direction isotropic load path used for fiber trajectory definition. Source: [3]

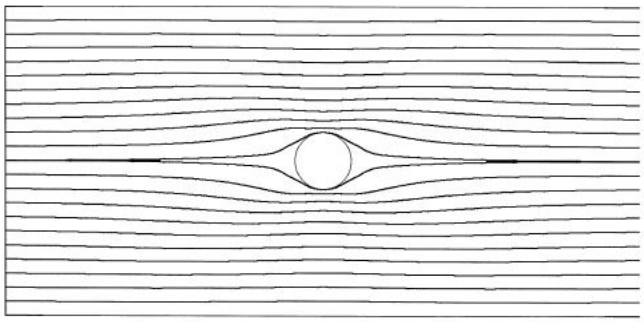

Figure 1.2: X-direction anisotropic load path used for fiber trajectory definition. Source: [3]

The fiber trajectories obtained using the load path of the structure are shown to be similar, in terms of overall shape, to those derived from principal stress directions. However, an important distinction emerges: the trajectories obtained from the load path method are globally smoother and straighter and exhibit larger minimum steering radii. These characteristics are particularly relevant from a manufacturing perspective, as they reduce fiber waviness and facilitate the practical realization of steered laminates. Moreover, as illustrated in Figure 1.1 and Figure 1.2, load paths generated under different load magnitudes acting along the same direction lead to similar fiber configurations. This observation highlights the robustness of the approach presented with respect to variations in loading conditions. At the same time, the resulting fiber trajectories remain continuous throughout the structure and are never interrupted in the vicinity of the cutout, ensuring uninterrupted load transfer around the hole and avoiding premature termination of the fibers.

A further key difference between the two studies lies in the scope of validation. While the work proposed by Hyer is limited to numerical analyses, Tosh and Kelly extend the

investigation to include both analytical and experimental results. The authors develop manufacturing techniques capable of producing laminates with steered fiber trajectories and subsequently perform mechanical testing. Tensile tests on open hole specimens and bearing tests on pin loaded configurations are conducted under displacement controlled conditions, allowing a direct experimental assessment of the effectiveness of the load path based design strategy. The manufactured laminates differed in stacking sequence, the possible presence of tow overlap, and the number of steered plies. These variations were examined to evaluate the influence of load path based plies on the mechanical response. The experimental results were then compared with those obtained for a straight fiber laminate, which served as the baseline configuration.

With regard to the tensile tests, load path based laminates allowing tow overlap exhibited an approximately linear increase in load carrying capacity with respect to the baseline laminate, in particular strength increases of approximately 20, 40, and 60 percent were observed for laminates containing one, two, and three steered plies, respectively. Load path based laminates designed to avoid tow overlap showed a slightly different behavior in fact their strength remained higher than that of the baseline laminate and no splitting along the fiber direction was observed, despite the limited transverse reinforcement. These results suggest that the quasi isotropic base laminate could potentially be omitted however, doing so would render the structure more susceptible to undesirable failure modes, such as transverse compressive or stability driven failures.

Conventional straight fiber composite laminates are typically designed to resist a single dominant failure mode; however, due to the combined nature of the stresses acting around a pin loaded hole, these traditional designs often fail to exploit the full potential of the reinforcing fibers. In particular, aligning fibers with a single principal stress direction may improve resistance to one load component while leaving other critical load paths insufficiently supported. Within this context, the application of fiber steering strategies to pin loaded laminates was investigated, with the aim of improving load transfer efficiency and increasing the overall load carrying capacity of mechanically fastened joints. By extending the load path based design concept to pin loaded configurations, the study seeks to capture the global flow of load from the pin into the surrounding laminate and to evaluate whether this approach can provide advantages over designs based solely on principal stress directions. The bearing test results highlight clear differences in the load carrying capability of the four laminate categories investigated, as shown in Figure 1.3.

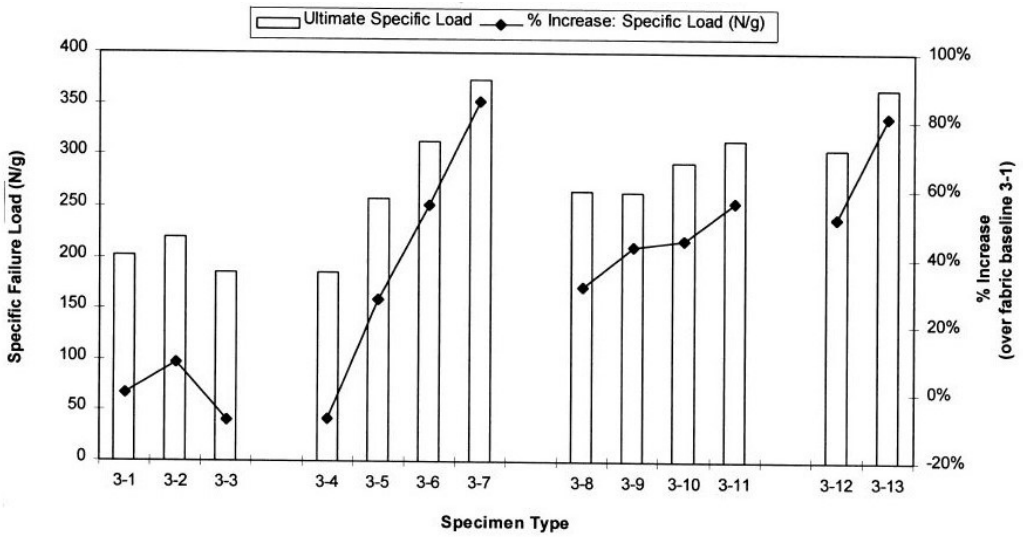

Figure 1.3: Bearing load test results. Source: [3]

Conventional straight-fiber baseline laminates exhibit the lowest bearing strength, with failure dominated by localized compressive damage at the pin–hole interface, reflecting inefficient load transfer from the pin into the laminate. Laminates designed using fibers aligned with principal tensile stress directions show a moderate improvement in bearing performance; however, their effectiveness is limited, as this approach primarily enhances resistance to net-section tension while providing insufficient support for the compressive contact stresses generated by the pin. In contrast, laminates incorporating fibers aligned with principal compressive stress directions demonstrate a further increase in bearing load capacity, indicating improved resistance to compression. Nevertheless, these laminates remain constrained by the absence of a complementary tensile mechanism able to carry the load. The highest bearing strengths are achieved by load path based and hybrid laminate configurations, which exhibit substantial improvements relative to the baseline. By following the global flow of load from the pin into the surrounding laminate, these fiber architectures effectively accommodate both tensile and compressive load components, leading to delayed damage initiation and a more distributed bearing stress field. Hybrid designs achieve nearly the same level of performance as fully steered configurations while requiring fewer steered plies, underscoring the effectiveness of load path based design strategies in capturing the true mechanics of pin loaded composite joints. While these results clearly demonstrate the structural benefits of fiber steering based on load path, they also emphasize that physically driven design approaches are inherently dependent on the specific case under consideration. In order to extend these concepts beyond individual case studies and enable a systematic and generalizable design methodology, a more formal mathematical framework is required.

1.2. Computational and manufacturing approaches to variable stiffness laminates

In his work, Tatting [4] integrates manufacturing considerations directly into the design process by coupling the finite element model with a spatially varying stacking sequence. The laminate architecture is allowed to vary as a function of position due to the presence of plies manufactured by tow placement, thereby explicitly accounting for the effects of fiber steering on the structural response. The optimized steered laminates are subsequently manufactured and experimentally tested, providing validation of the proposed design methodology. This approach represents a clear transition from laminates designed according to the load path method to optimization based steered laminates, fundamentally changing the design process.

The methodology adopted by Tosh and Kelly is primarily physical in nature. After analyzing how the structure transfers load, fibers are placed so as to follow the observed load paths. This strategy requires tailoring specific to each case and cannot be readily generalized to arbitrary geometries or loading conditions. In contrast, Tatting proposes a mathematical framework based on optimization, in which fiber orientations are treated as design variables. Given a limited set of input parameters and constraints, this approach can be systematically applied to a wide range of structures, enabling the automated generation of steered laminate designs that are both structurally efficient and manufacturable.

Within this context, manufacturing constraints are explicitly integrated into the design process in order to ensure the feasibility of the resulting panels. One of the most relevant constraints is the minimum allowable curvature radius of the tow placement head, which must be properly accounted for. If this constraint is violated, the manufactured panel may deviate from planarity, leading to imperfections and a consequent degradation of the load bearing capability of the structure. After careful consideration, the design variables were selected as follows:

$$
\begin{aligned}
(x_0, y_0) &\longrightarrow \text{coordinates of the origin of the reference path} \\
T_0 &\longrightarrow \text{fiber orientation angle of the reference path at the origin} \\
\phi &\longrightarrow \text{angle representing the major direction of variation} \\
d &\longrightarrow \text{characteristic length in } \phi\text{-direction} \\
T_1 &\longrightarrow \text{fiber orientation angle of the reference path at } d
\end{aligned}
$$

The parameters just discussed provide a general description of the so called linear angle variation, a particular reference path, that satisfies the Equation (1.1).

$$\theta(r) = \begin{cases} \phi + T_0 + \dfrac{(T_1 - T_0)}{d}\, r, & 0 < r < d, \\ \phi + T_1 + \dfrac{(T_0 - T_1)}{d}\, (r - d), & d < r < 2d. \end{cases} \tag{1.1}$$

In this context, r is the coordinate in ϕ-direction, $\theta(r)$ is periodic and continuous in the domain with a period of $2d$ and has a limit T_0 and T_1 moreover the curvature radius can be found analytically and compared with the minimum radius of the machine used. The tow are deposited normal to the ϕ-direction but, due to the curvature of the tows, there can be gaps or overlap so two different techniques are developed which are the tow drop the overlap.

The tow drop method defines a manufacturing strategy in which the tow placement machine is instructed to discontinue individual tows whenever overlaps would arise as a consequence of differing fiber trajectories. By selectively cutting and dropping tows during the deposition process, this method ensures that the laminate maintains a constant thickness throughout the entire structure however, this approach inherently allows the presence of gaps within the panel. These gaps correspond to area that do not contain fibers and arise between adjacent courses; nevertheless, because neighboring tows generally exhibit similar fiber orientations, the geometric extent of these regions is limited and their impact on the overall structural behavior is reduced.

The overlap method, on the other hand, permits contiguous tows to overlap during deposition, leading to localized accumulations of material and, consequently, to variations in laminate thickness across the panel. The degree of overlap is governed by a dedicated parameter, commonly referred to as the overlap parameter, which provides direct control over the balance between material accumulation and gap formation. This parameter varies continuously between zero and one. A value of zero corresponds to the so called *no-overlap* configuration, in which adjacent tows are allowed to come into contact without overlapping, resulting in the formation of gaps within the structure. Conversely, a value of one defines the *no-gap* configuration, where sufficient overlap is introduced to completely eliminate regions without fibers, at the cost of increased local thickness. Intermediate values of the overlap parameter allow a gradual transition between these two extremes, enabling a continuous modulation of both overlap and gap distribution within the laminate.

The flexibility provided by the overlap parameter yields a broad design space that can be

systematically explored to evaluate the effectiveness of stiffness tailoring through curvilinear fiber placement. Representative examples of panels manufactured using the tow drop and overlap methods are shown in Figure 1.4 and Figure 1.5, respectively.

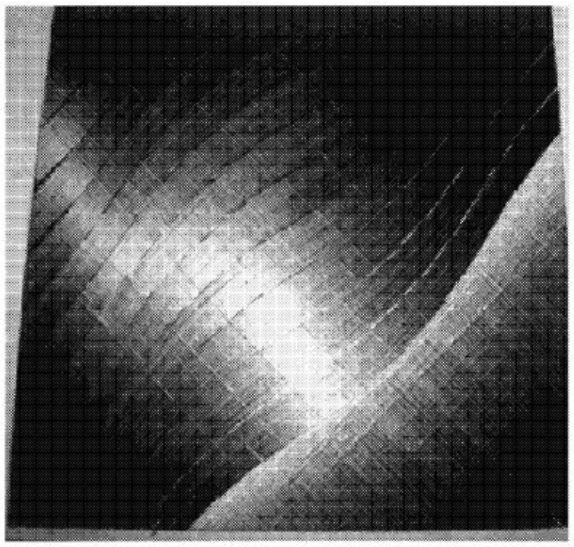

Figure 1.4: Fabricated panel using the tow drop method. Source: [4]

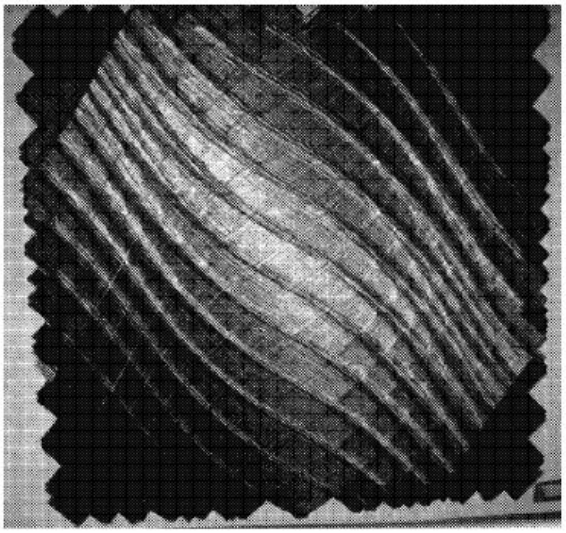

Figure 1.5: Fabricated panel using the overlap method. Source: [4]

In conventional finite element models of composite laminates, each element is typically assigned an identical stacking sequence throughout the structure but this assumption is no longer valid in the presence of curvilinear fiber layouts, where the laminate architecture varies spatially due to fiber steering. In this study, the stacking sequence at any point within the structure can be determined through a set of design parameters and the governing equations introduced previously. This capability enables the transformation of a generic finite element model into a tow-steered laminate representation.

To automate the definition of tow-steered laminates, Tatting developed the Laminate Definition Tool (LDT), which takes as input the total number of plies together with the relevant design parameters and determines the local stacking sequence at the centroid of each finite element. The resulting ply level information is directly linked to the finite element model, enabling an accurate representation of the spatial variation of fiber orientations and while this approach provides a detailed and consistent description of tow-steered laminates, it relies on iterative calculations and can become computationally demanding when a large number of configurations must be evaluated.

To address this limitation, the author introduced the Optimal Laminate Geometry Analysis (OLGA) software as a high level design tool intended for preliminary laminate optimization. Unlike the LDT, OLGA does not explicitly define the stacking sequence, but

instead describes the laminate through spatially varying equivalent stiffness properties. By treating these properties as continuous design variables, OLGA enables efficient optimization of the structural response under given loading and boundary conditions, making it particularly suitable for early stage design studies. Once an optimal distribution of laminate properties has been identified, the corresponding tow-steered laminate can be realized through subsequent ply level discretization using the Laminate Definition Tool. In this way, OLGA and LDT operate in a complementary manner, combining computational efficiency during the preliminary design stage with a detailed laminate definition that accounts for manufacturing aspects.

In this study, a total of forty five laminate configurations were investigated. These included five constant stiffness designs used as baseline configurations, five laminates with steered fibers designed using the tow drop method, and five laminates with steered fibers designed using the overlap method. Each of these fifteen laminate architectures was analyzed using finite element models with different hole diameters, resulting in a comprehensive parametric investigation of the influence of fiber steering and geometric discontinuities on structural performance. For the straight fiber laminates, the definition of the stacking sequence was straightforward, as the lay up remained uniform throughout the structure. In contrast, for the laminates with steered fibers, the stacking sequence varied spatially as a consequence of fiber steering and in these cases, the Laminate Definition Tool was employed to determine the local stacking sequence at the centroid of each finite element, ensuring an accurate representation of the steered laminate architecture within the finite element framework.

The compressive response of the laminates was evaluated through axial compression tests performed on flat rectangular panels, with and without a central circular hole. The specimens were loaded under displacement controlled conditions to ensure stable test execution and consistency with the numerical analyses. The upper and lower edges of each panel were potted to enforce clamped boundary conditions, allowing uniform load introduction along the compression direction. To prevent premature out of plane instability while preserving realistic in plane behavior, the lateral edges of the specimens were supported using knife edge constraints, which restricted out of plane displacements without inhibiting in plane motion. This boundary condition configuration was selected to closely replicate the assumptions adopted in the finite element models and to enable a direct comparison between experimental measurements and numerical predictions. The primary quantities of interest were the global load displacement response and the critical buckling load, which were used to assess the influence of tow steering, hole size, and laminate architecture on compressive stability. The results obtained from these compression tests are presented

and discussed in Figure 1.6.

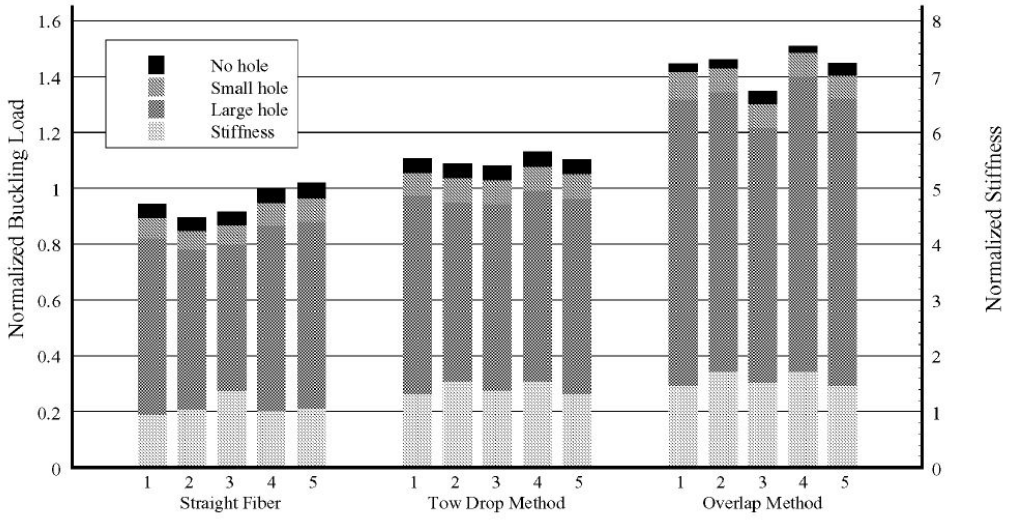

Figure 1.6: Result of the compression tests. Source: [4]

From the graph, several observations can be drawn. The presence of a central hole results in a consistent reduction of the compressive performance for all laminate configurations. In particular, a decrease of approximately 5.5 percent is observed for panels with a small hole, while a larger reduction of about 13.5 percent occurs for panels with a large hole, irrespective of the laminate architecture. Despite this degradation, laminates with steered fibers consistently exhibit higher buckling loads than the baseline configurations. In particular, the buckling load increases by approximately 20 percent for laminates manufactured using the tow drop method and by up to 60 percent for those produced using the overlap method. These results indicate that the local thickness build up associated with curvilinear fiber placement promotes a more favorable redistribution of the applied load, shifting it away from thinner regions toward areas with increased stiffness. This mechanism, combined with the enhanced bending stiffness induced by the thickness variations, leads to a significant improvement in buckling resistance and reduces the sensitivity of the structure to geometric discontinuities such as holes.

The works of Tosh and Kelly and Tatting address the common objective of enhancing the structural efficiency of composite laminates through fiber steering, while approaching the problem at different levels of abstraction. They focus on the physical mechanisms governing load transfer, providing experimental evidence that aligning fibers with global load paths can significantly improve strength and stability, particularly in the presence of stress concentrations. Their contribution establishes the physical validity and structural potential of load path based fiber steering. Building upon this physical foundation, Tatting

introduces a systematic design framework based on mathematical optimization, enabling the generation of steered laminate architectures in a general and automated manner. Rather than targeting individual configurations, his work formalizes fiber steering as a set of design variables subject to manufacturing constraints, thereby extending physically driven concepts into a scalable and producible design methodology supported by both numerical and experimental validation.

Considered together, these studies delineate a clear progression from physically motivated design intuition toward optimization based, manufacturing aware approaches for tow steered composite structures. While Tosh and Kelly provide the experimental support underlying fiber steering, Tatting supplies the computational tools required to translate this rationale into a generalized design framework, thereby paving the way for subsequent developments in variable stiffness laminate optimization.

Following the framework introduced by Tatting, subsequent research shifted from the definition of individual tow-steered designs toward a more fundamental investigation of the structural response of laminates with spatially varying stiffness. In this context, the work of Gürdal and al. [5] represents a natural extension of the preceding studies, as it focuses on the mechanics and performance implications of variable stiffness laminates rather than on specific load path configurations.

While earlier contributions demonstrated the feasibility and advantages of fiber steering through physically motivated designs and numerical optimization, the present study systematically investigates how prescribed stiffness variations affect the in plane stress distribution, buckling response, and the trade off between global stiffness and structural stability in composite panels. By introducing simplified yet general descriptions of fiber orientation variation and analyzing their effects under compressive loading, this work provides deeper insight into the fundamental mechanisms responsible for the enhanced buckling performance observed in tow steered laminates. As such, it consolidates the transition from case specific design strategies to a more general theoretical understanding of variable stiffness composite structures.

The study is primarily concerned with developing a fundamental mechanical understanding of the effects induced by spatially varying laminate stiffness in composite panels. Rather than focusing on the generation of optimal fiber trajectories, the authors deliberately prescribe the fiber orientation field in order to isolate and investigate the structural consequences of stiffness variation. This choice allows the effects of fiber steering to be studied independently of specific optimization strategies or load path derivation techniques. The spatial variation of the fiber orientation is defined with respect to a reference

coordinate system, and its formulation follows a two stage formulation. Initially, the fiber orientation angle is expressed in the global coordinate system (x, y), where the x-axis denotes the direction along which the orientation variation is prescribed. Subsequently, the formulation is generalized by introducing a rotated coordinate system, obtained by rotating the global axes by an angle ϕ, in order to allow the direction of stiffness variation to assume an arbitrary orientation within the panel plane. In the rotated coordinate system, the fiber orientation angle is defined as a function of the local coordinate x', and is expressed through a linear angle variation law as:

$$\theta(x') = \phi + T_0 + \frac{T_1 - T_0}{d} |x'| \tag{1.2}$$

where T_0 and T_1 denote the fiber orientation angles at the center and at the edge of the panel, respectively, x' is the coordinate measured along the direction of variation in the rotated reference frame, and d represents a characteristic distance. This formulation ensures symmetry of the fiber orientation field with respect to the panel center and enables a continuous variation of the fiber angle from the mid-plane toward the boundaries. The introduction of the rotation angle ϕ decouples the direction of stiffness variation from the global coordinate system, allowing it to be aligned with an arbitrary structural direction. As in the formulation introduced by Tatting for tow steered laminate design, a linear angle variation law is adopted to describe curvilinear fiber paths however, in the work of Gürdal et al., this law is prescribed not as part of an optimization framework, but as a means to investigate the fundamental mechanical implications of spatial stiffness variation.

The local fiber orientation $\theta(x')$ is then transformed into the global coordinate system through ϕ, enabling evaluation of the laminate stiffness matrices in the global reference frame. Since the fiber angle varies continuously with position, the transformed reduced stiffness matrix of each ply, $\bar{\mathbf{Q}}(\theta)$, becomes spatially dependent. Consequently, the laminate extensional and bending stiffness matrices are no longer constant throughout the structure, but vary as functions of the spatial coordinates, so:

$$\mathbf{A} = \mathbf{A}(x, y), \qquad \mathbf{D} = \mathbf{D}(x, y).$$

This spatial dependence of the laminate stiffness matrices represents the defining characteristic of variable stiffness laminates and constitutes the central focus of the study. To investigate its effects, the authors consider a set of representative flat composite panels subjected to in plane loading and axial compression, comparing constant stiffness laminates with variable stiffness configurations generated through prescribed fiber orientation

laws. The selected case studies are deliberately simple in geometry and boundary conditions, in order to isolate the mechanical effects of stiffness variation from geometric or loading complexities. For the variable stiffness cases analyzed, the spatial variation of $\mathbf{A}$ leads to a redistribution of membrane stresses that differs significantly from that observed in constant stiffness laminates. Regions characterized by locally increased stiffness in the direction of the applied load attract a larger share of the in plane forces, while regions with lower stiffness experience reduced stress levels. This mechanism results in smoother stress gradients and lower peak stresses across the panel. Although this behavior is conceptually similar to the load redistribution observed in load path based laminates, in the present study it arises naturally from the prescribed spatial variation of the laminate stiffness matrices, without the need to explicitly construct fiber trajectories based on stress flow. The influence of stiffness variation becomes even more pronounced when considering the stability behavior under compressive loading. In constant stiffness laminates, the bending stiffness matrix $\mathbf{D}$ is uniform, and the buckling response is primarily governed by the panel geometry and the applied boundary conditions. The corresponding buckling mode shapes reflect this uniformity, and the critical buckling load is limited by the least stiff regions of the structure.

In contrast, for variable stiffness laminates, the spatial dependence of the bending stiffness matrix $\mathbf{D}(x, y)$ fundamentally alters the buckling problem. The governing stability equations now involve spatially dependent stiffness terms, leading to buckling modes that are strongly influenced by the underlying stiffness distribution. The numerical results presented in the paper show that these modified mode shapes tend to localize deformation in regions of lower bending stiffness, while stiffer regions effectively constrain the out of plane displacement. As a consequence, the global buckling behavior is delayed and the critical buckling load is significantly increased. To support the parametric investigation, the authors introduce a set of representative case studies designed to progressively highlight the effects of stiffness variation on the buckling behavior of composite panels. These cases, denoted as Case I(a), Case I(b), and Case II, are formulated to separate the influence of fiber orientation variation from geometric and loading effects, while maintaining a clear comparison with constant stiffness baseline configurations. Figure 1.7 illustrates the deformation of the laminates corresponding to the previously described cases under uniform end shortening.

In Case I(a), the panel is subjected to uniaxial compressive loading, and the fiber orientation variation is prescribed along the loading direction. This configuration represents the most direct application of stiffness tailoring, as the variation of the fiber angle directly affects both the extensional stiffness in the load direction and the bending stiffness govern-

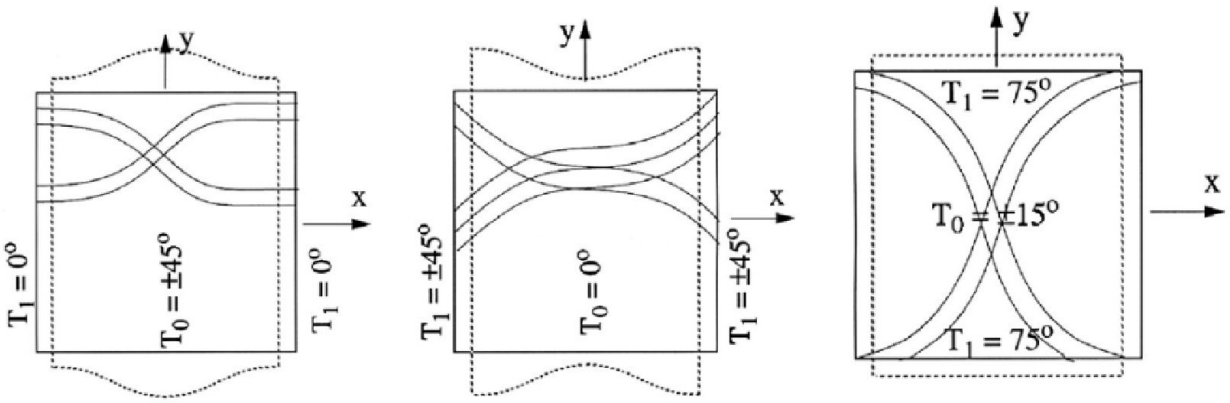

Figure 1.7: In-plane deformations of the the laminates under uniform end shortening. Source: [5]

ing stability. The results show that increasing the gradient of fiber orientation variation leads to a noticeable increase in the critical buckling load. This improvement is attributed to the enhancement of bending stiffness in regions that are most susceptible to instability, which modifies the buckling mode shape and delays the onset of global buckling. Importantly, the increase in buckling load is achieved without any change in laminate thickness or mass, confirming that the performance gains arise solely from stiffness redistribution.

Case I(b) extends the previous configuration by prescribing the fiber orientation variation along a direction that is not aligned with the applied compressive load. By introducing a rotation angle ϕ between the direction of stiffness variation and the global loading direction, this case investigates the sensitivity of the buckling response to the orientation of the stiffness gradient. The results indicate that the effectiveness of stiffness tailoring depends strongly on the alignment between the stiffness variation and the dominant buckling mode. When the stiffness gradient is favorably aligned with the deformation pattern, significant improvements in buckling performance are retained. Conversely, misalignment between the stiffness distribution and the buckling mode reduces the effectiveness of stiffness tailoring, leading to smaller gains compared to Case I(a). This case demonstrates that, although fiber steering does not require a unique optimal trajectory, the directionality of stiffness variation plays a critical role in determining the resulting stability improvements.

Case II further generalizes the analysis by considering panels subjected to biaxial compressive loading, thereby introducing a more complex stress state representative of realistic structural applications. In this configuration, stiffness tailoring must simultaneously interact with multiple load components and associated deformation mechanisms. The results show that variable stiffness laminates continue to outperform constant stiffness configura-

tions under biaxial loading; however, the magnitude of the improvement depends on how the spatial stiffness distribution interacts with the combined buckling modes activated by the applied loads. Rather than enhancing stiffness along a single preferred direction, effective performance gains in this case are obtained through a balanced redistribution of bending stiffness capable of supporting multiple instability mechanisms concurrently. This behavior highlights that, under complex loading conditions, the benefits of stiffness tailoring arise from a coherent modulation of the bending stiffness field rather than from aggressive tailoring aligned with a single load component. Figure 1.8 illustrates the variation of buckling load and stiffness as a function of T_0 compared to the baseline configuration.

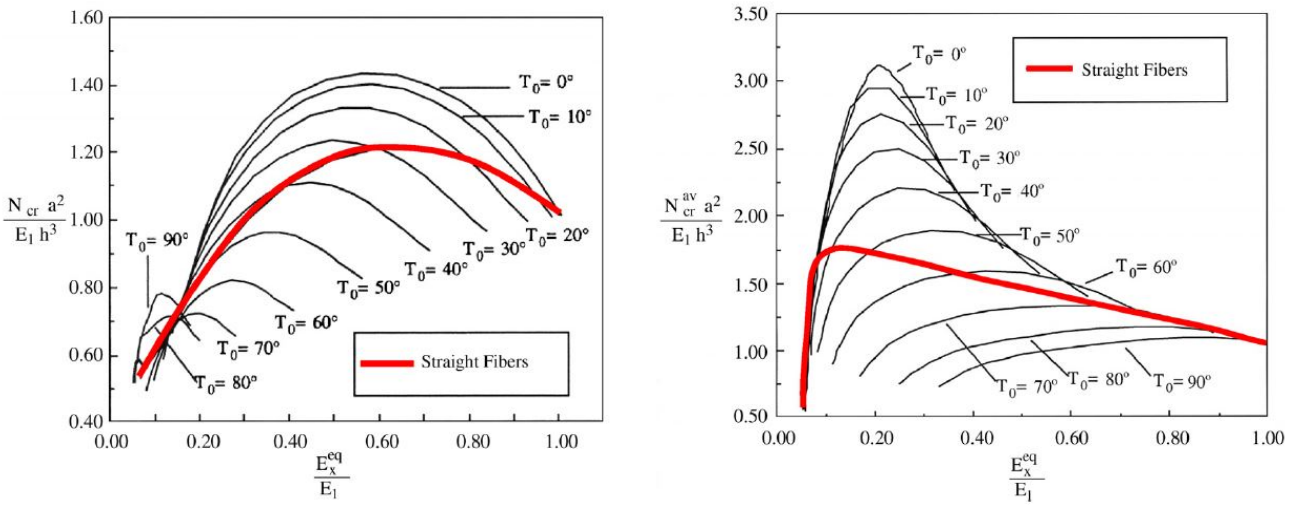

(a) Case I laminate

(b) Case II laminate

Figure 1.8: Buckling and stiffness performance under uniform end shortening. Source: [5]

While this analysis establishes a clear mechanical understanding of how spatial stiffness variation influences buckling behavior, it also brings into focus the inherent limitations of approaches based on prescribed orientation laws and isolated parametric investigations. Although such methods are effective in elucidating the fundamental mechanics of variable stiffness laminates, they do not provide a systematic procedure for identifying optimal stiffness distributions when extended to complex geometries, diverse loading environments, and realistic design constraints.

In this context, the work by Setoodeh et al. [6] represents a natural and necessary progression from descriptive and parametric studies toward a fully design methodology based on optimization. Building upon the mechanical insights developed in earlier investigations, the authors address the complementary problem of how variable stiffness distributions can be systematically generated with the explicit objective of maximizing the critical buckling load. To this end, fiber orientation angles are treated as continuous design variables defined at the finite element nodal level, allowing both the extensional and bending stiffness properties of the laminate to vary spatially across the panel in a controlled and systematic manner. The resulting optimization problem is formulated directly in terms of the buckling eigenvalue and is solved using a generalized reciprocal approximation expressed in terms of the laminate compliance tensors. This formulation enables the decomposition of the global design problem into a set of local optimization subproblems, thereby significantly improving computational efficiency and making the approach particularly well suited for large-scale variable stiffness laminate design. Unlike earlier methodologies based on predefined fiber orientation laws, the optimal stiffness distribution in this framework emerges naturally from the solution of the optimization problem, subject to equilibrium, stability, and constraints related to the manufacture process.

The most relevant contribution of this work is the generalized reciprocal approximation is introduced for the optimization of variable stiffness composite panels with respect to buckling performance. In composite laminates stiffness is not described by a scalar quantity but rather by the extensional and bending stiffness matrices, $\mathbf{A}$ and $\mathbf{D}$, which depend locally on the fiber orientation. To extend the reciprocal approximation concept to this context, the authors reformulate the problem in terms of the laminate compliance tensors, defined as

$$\mathbf{R} = \mathbf{A}^{-1}, \qquad \mathbf{S} = \mathbf{D}^{-1}.$$

This transformation enables the buckling eigenvalue to be expressed as a function of the local compliance components, rather than directly in terms of fiber orientation angles. The critical buckling load is obtained from the generalized eigenvalue problem

$$(\mathbf{K}_b - \lambda \mathbf{K}_g)\,\mathbf{a} = \mathbf{0} \tag{1.3}$$

where $\mathbf{K}_b$ is the global bending stiffness matrix, $\mathbf{K}_g$ is the geometric stiffness matrix associated with the in plane stress state, λ is the critical buckling load factor, and $\mathbf{a}$ is the corresponding buckling mode shape. The sensitivity of the buckling eigenvalue with respect to variations in the local compliance tensors is evaluated using the chain rule. For a generic finite element e, the derivative of the buckling load with respect to the bending

compliance tensor is expressed as:

$$\frac{\partial \lambda}{\partial \mathbf{S}_e} = \frac{\partial \lambda}{\partial \mathbf{D}_e} \cdot \frac{\partial \mathbf{D}_e}{\partial \mathbf{S}_e} \tag{1.4}$$

Since $\mathbf{S}_e = \mathbf{D}_e^{-1}$, the above expression becomes

$$\frac{\partial \lambda}{\partial \mathbf{S}_e} = -\mathbf{D}_e \cdot \frac{\partial \lambda}{\partial \mathbf{D}_e} \cdot \mathbf{D}_e \tag{1.5}$$

An analogous formulation is obtained for the extensional compliance tensor $\mathbf{R}_e$,

$$\frac{\partial \lambda}{\partial \mathbf{R}_e} = -\mathbf{A}_e \cdot \frac{\partial \lambda}{\partial \mathbf{A}_e} \cdot \mathbf{A}_e \tag{1.6}$$

A key advantage of this formulation lies in the spatial separability of the reciprocal approximation. The variation of the buckling eigenvalue can be expressed as a summation of local contributions associated with individual finite elements, allowing the global optimization problem to be decomposed into a set of independent local subproblems. This represents a fundamental shift from optimization strategies based on prescribed fiber orientation laws and establishes the mathematical foundation for efficient large scale optimization of variable stiffness laminates. This decomposition is explicitly reflected in the sensitivity expression of the critical buckling load reported in the equation below.

$$\frac{d\lambda}{d\mathbf{b}} = \mathbf{a}^{\mathrm{T}} \cdot \left(\frac{d\mathbf{K}^b}{d\mathbf{b}} - \frac{d\mathbf{K}^g}{d\mathbf{b}} \right) \cdot \mathbf{a} \tag{1.7}$$

The total variation is separated into two distinct contributions. The first term is associated with variations of the bending stiffness matrix and captures the direct influence of local stiffness modifications on the structural response while the second term arises from the dependence of the geometric stiffness matrix on the in-plane stress state, which is indirectly affected by changes in the laminate extensional properties.

An important aspect emerging from the numerical results is that, within the proposed optimization framework, the fiber orientation is treated as a continuous design variable rather than as a discretely prescribed quantity. The orientation angle is defined at the finite element nodal level and interpolated within each element, allowing it to vary smoothly across the panel. As a consequence, the optimized solutions obtained from the numerical procedure represent continuous stiffness distributions, rather than explicitly defined fiber paths or discrete tow trajectories. This continuous representation enables the optimiza-

tion algorithm to explore the full space of admissible stiffness variations without being restricted by predefined orientation laws or discrete angle sets.

The critical buckling load factor λ is calculated at each iteration by exploiting the generalized buckling eigenvalue problem associated with the bending and geometric stiffness matrices. The sensitivity of λ with respect to the local design variables is evaluated using the reciprocal approximation framework, which provides an efficient estimate of how incremental changes in the laminate stiffness properties affect the global stability response. By leveraging the sensitivity of the variable, the variation of the buckling load factor can be approximated without requiring the solution of a full eigenvalue problem at every design update. This strategy significantly reduces the computational cost of the optimization process and makes the approach suitable for large scale variable stiffness laminate problems involving a large number of design variables. Figure 1.9 shows the convergence history for a panel subjected to unidirectional loading, comparing the cases of simply supported and clamped boundary conditions.

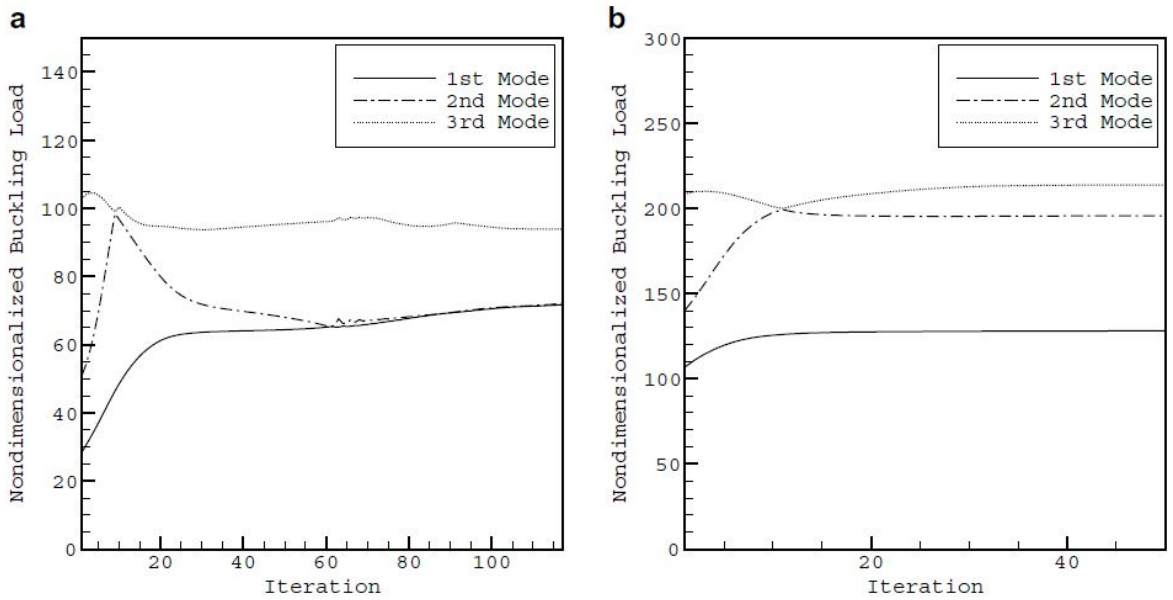

Figure 1.9: Iteration history for a square plate under uni-directional buckling (a) simply supported (b) clamped. Source: [6]

The resulting optimization procedure remains directly governed by the underlying buckling equations throughout the design process. At each iteration, the structural equilibrium and stability conditions are satisfied implicitly through the finite element analyses used to evaluate the in plane stress state and the corresponding buckling response. Constraints on the spatial variation of stiffness are enforced through smoothing techniques applied to the compliance fields, which limit abrupt changes in the local stiffness properties and

ensure a physically meaningful variation of fiber orientation across the panel. This regularization plays a crucial role in maintaining numerical stability during the optimization process and in producing stiffness distributions that can be interpreted mechanically as continuous stiffness tailoring solutions.

The numerical results presented in the final section of the paper quantitatively confirm the effectiveness of the proposed optimization approach. For all configurations examined, variable stiffness laminates exhibit higher critical buckling loads than the corresponding constant stiffness baseline designs, while maintaining the same laminate thickness and mass. The results show that the degree of buckling enhancement is strongly influenced by the boundary conditions. In simply supported panels, where the buckling response is governed primarily by the spatial distribution of bending stiffness, stiffness tailoring leads to pronounced modifications of the buckling mode shapes and to substantial increases in the critical load. In contrast, for clamped panels, the inherent stabilizing effect of the boundary constraints reduces the relative sensitivity of the buckling response to stiffness redistribution, resulting in smaller but still significant performance gains, as shown in Table 1.2.

Table 1.2: Critical buckling loads associated with the first three buckling eigenvalues for the baseline and optimized variable stiffness laminate configurations. Source: [6]

	Buckling eigenvalues			
Configuration	N_1	N_2	N_3	Improvement
Simply supported				
Constant stiffness	28.50	50.98	102.75	–
Optimized variable stiffness	75.68	76.64	92.07	165.58
Clamped				
Constant stiffness	106.87	140.32	208.52	–
Optimized variable stiffness	136.46	160.22	203.76	27.70

These results indicate that the optimization framework is capable of exploiting stiffness redistribution most effectively in configurations where the buckling response is highly sensitive to the spatial distribution of bending stiffness. Moreover, the consistent improvement observed across different loading scenarios confirms that the enhanced stability performance does not arise from a single configuration dependent stiffness pattern, but rather from a systematic tailoring of the laminate stiffness properties. This behavior demonstrates the robustness of the proposed approach and highlights its ability to improve buckling performance under a wide range of structural configurations.

Overall, the numerical examples demonstrate that treating fiber orientation as a con-

tinuous design variable allows the full stiffness tailoring potential of fiber steering to be exploited. The optimized solutions obtained in this manner define idealized target stiffness distributions that represent a theoretical upper bound on the achievable buckling performance of composite panels. These assumptions leads to have perfectly smooth and continuous fiber paths but, in practice, the realization of such target stiffness distributions requires the discretization of the fiber layout into a finite number of tows deposited using automated fiber placement technologies. This type of process introduces unavoidable local deviations from the idealized stiffness field introducing characteristic features of the manufacturing process, such as local tow gaps and overlaps. These features represent a direct consequence of translating continuous fiber orientation fields into manufacturable tow based laminates and cannot be eliminated without compromising the intended stiffness distribution so, as a result, the presence of these defects becomes a critical factor in determining the actual structural response of variable stiffness laminates.

1.3. Effects of gaps and overlaps in variable stiffness laminates

In this context, the work by Fayazbakhsh et al. [12] addresses the need to incorporate manufacturing induced imperfections into the mechanical analysis of variable stiffness composite panels by proposing a modeling framework capable of capturing the influence of gaps and overlaps on their buckling behavior. In earlier studies, such as that by Blom et al. [7], manufacturing defects were taken into account however, their representation was typically binary. Finite elements were assumed to be either entirely composed of sound composite material or fully occupied by a defect region and although this approach allows the presence of defects to be identified, it requires extremely fine finite element meshes to accurately capture their geometry and spatial distribution, leading to a significant increase in computational cost and a reduction in modeling efficiency.

To overcome these limitations, the authors introduce the defect layer method, which provides a more realistic and computationally efficient description of manufacturing defects. A key aspect of this approach is the recognition that defects in laminates produced with Automatic Fiber Placement (AFP) are not inherently binary in fact they found that a given ply, or even a finite element within a ply, may be only partially affected by gaps or overlaps. This behavior is captured through the introduction of the defect area percentage, defined as the ratio between the defective area and the total area of a given layer within a finite element. This parameter enables a continuous description of the defect state, ranging from a defect free condition to a fully defective layer.

Based on this parameter, the mechanical properties or thickness of each layer are modified accordingly. In the case of gap-modified defect layers, the increasing presence of resin rich regions leads to a progressive reduction of the effective elastic properties. These reduced properties are not assumed a priori but are obtained through detailed finite element analyses performed on representative single layer specimens containing gaps of varying extent. The resulting elastic moduli are then expressed as continuous functions of the defect extent and used to characterize the mechanical response of gap-modified layers. Conversely, for overlap-modified defect layers, the elastic properties are assumed to remain identical to those of the pristine composite material, while the effective thickness of the layer is increased proportionally to the overlap extent. Once the defect sensitive material properties are defined, the finite element model of the variable stiffness laminate is constructed analytically. The local fiber orientation within each finite element is determined using the follow expression

$$\sin \varphi = \sin (T_0) + k|x| \tag{1.8}$$

It shows how the variable φ is function of the angle orientation at the center of the plate T_0 and the curvature k of the fiber. The locations of gaps and overlaps are identified through dedicated numerical routines that simulate the AFP manufacturing process by accounting for tow additions and drops between adjacent courses.

For each ply and each finite element, the intersection between the element area and the defect regions is evaluated, allowing the local extent of defects to be quantified. The resulting defect area percentage constitutes the key link between manufacturing effects and structural analysis as it is used to assign the appropriate elastic properties and, in the case of overlaps, the effective layer thickness within the finite element formulation.

The method developed for locating manufacturing defects proved to be highly accurate and it was shown to be independent of the finite element size adopted in the numerical models, thereby overcoming the main problem encountered in previous studies, as shown in Figure 1.10. This aspect is particularly relevant for the analysis of large or complex structures, as it allows reliable defect characterization without the need for excessive mesh refinement.

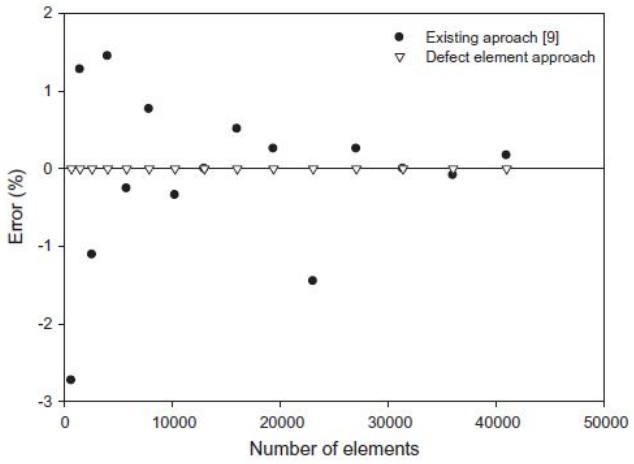

Figure 1.10: Error in calculating gap area percentage using the method proposed by Blom et al. and the defect layer method. Source: [12]

Following the evaluation of the elastic properties of the defect-modified layers, finite element models incorporating gaps and overlaps were constructed for both laminate designs under investigation. Numerical compression tests were then performed, and the resulting structural responses were compared with those of the baseline configuration in order to assess the influence of manufacturing defects on the critical buckling load and the in plane stiffness. This comparison made it possible to quantify the extent to which defects induced by automated fiber placement alter the mechanical benefits typically associated with variable stiffness design.

As shown in Table 1.3, the results consistently indicate that the presence of gaps leads to a deterioration of the in-plane stiffness in both designs; this reduction can be attributed to the introduction of resin rich regions, which exhibit a significantly lower load carrying capability compared to fiber reinforced material and therefore reduce the overall stiffness of the laminate. Moreover, the results demonstrate that even a relatively limited extent of gaps is sufficient to noticeably diminish the expected performance gains. In contrast, laminates incorporating overlaps exhibit a significant increase in buckling load. This behavior highlights the beneficial effect of local thickness build ups, which enhance the bending stiffness and improve the structural stability of variable stiffness composite panels under compressive loading.

The numerical framework proposed by Fayazbakhsh et al. (2013) represents a significant advancement in the analysis of variable stiffness laminates by explicitly accounting for manufacturing-induced defects. While the proposed approach proved to be both accurate and computationally efficient, the investigation remained purely numerical, leaving experimental validation as a necessary step to assess the applicability of the results to manufactured structures.

Building upon the numerical findings of Fayazbakhsh et al., the subsequent literature progressively shifts the focus from idealized modeling toward the investigation of manufacturing effects in real composite structures. In particular, the need to experimentally

Table 1.3: In-plane stiffness and buckling load after incorporating the effects of gaps or overlaps for designs (A) and (B), normalized with respect to the baseline laminate. Source: [12]

Laminate	Normalized stiffness		Normalized buckling load	
	Value	Change (%)	Value	Change (%)
Design (A)				
Ignoring defects	0.73	–	1.37	–
Full gap (12.4%)	0.61	-15.1	1.20	-12.4
Full overlap (9.6%)	0.78	+9.6	1.78	+29.9
Design (B)				
Ignoring defects	1.00	–	1.31	–
Full gap (12.3%)	0.86	-14.0	1.15	-12.2
Full overlap (9.4%)	1.11	+11.0	1.71	+30.5

validate the influence of gaps and overlaps, and to assess the extent to which numerical predictions remain reliable once manufacturing constraints are introduced, becomes increasingly evident. Within this context, the work of Marouene et al. [18] represents a key contribution, as it addresses the impact of defects induced by automated fiber placement from a manufacturing oriented perspective, thereby bridging numerical modeling and experimental assessment of variable stiffness composite panels.

The objective of the study is consistent with that of the previously discussed works, namely the investigation of the in plane stiffness and the critical buckling load through axial compression testing. The panels considered in the experimental campaign were symmetric and balanced laminates. The fiber trajectories defining the variable stiffness architecture were described by the following expression:

$$\cos\varphi = \cos\left(T_0\right) - k|x| \tag{1.9}$$

The parameters appearing in the expression are identical to those introduced in Equation (1.8). An example of a fiber trajectory with constant curvature is presented in Figure 1.11.

In the considered approach, gaps and overlaps are not treated as discrete geometric discontinuities within the laminate, but rather as regions characterized by modified local properties that can be found a priori by knowing the fiber steering law adopted.

The centerline of a reference course is first defined analytically as a function of the spatial coordinate x, as expressed in Equation (1.10). Based on this reference geometry, the lower boundary of the course is obtained by offsetting the centerline by half of the nominal course width, leading to the expression given in Equation (1.11). This formulation enables a precise geometric representation of the course boundaries while preserving the continuous description of the fiber orientation.

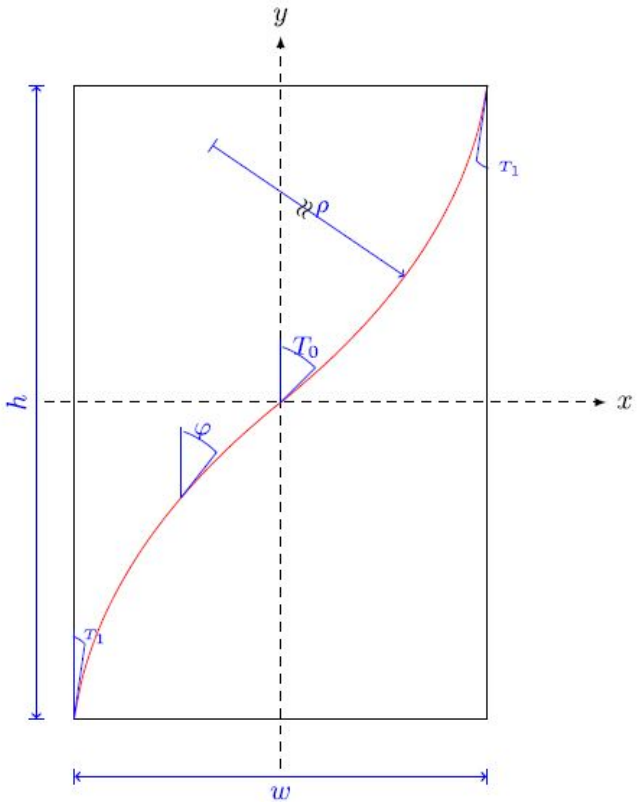

Figure 1.11: Reference path with a constant curvature. Source: [18]

The relative position of neighboring courses is then quantified through the definition of the distance D between adjacent course boundaries, as reported in Equation (1.12). This quantity provides a direct measure of the local spacing between courses and constitutes the key parameter for identifying the occurrence of gaps and overlaps. Specifically, positive values of D indicate the presence of gaps between adjacent courses, whereas negative values correspond to overlapping regions. This approach allows the extent and location of features arising from the manufacturing process to be evaluated prior to any discretization of the laminate into individual tows, thereby establishing a clear separation between the geometric definition of the fiber paths and their subsequent implementation within the automated fiber placement process.

$$y_{\text{centreline}} = \sqrt{\rho^2 - (x - \rho\cos T_0)^2} - \rho\sin T_0, \qquad -\frac{a}{2} \leq x < 0 \tag{1.10}$$

$$y_{\text{lower}} = \sqrt{\left(\rho - \frac{W_{\text{course}}}{2}\right)^2 - (x - \rho\cos T_0)^2} - \rho\sin T_0, \qquad -\frac{a}{2} \leq x < 0 \tag{1.11}$$

$$D = 2\left(-\sqrt{\left(\rho - \frac{W_{\text{course}}}{2}\right)^2 - (x - \rho\cos T_0)^2} + \rho\sin T_0\right), \qquad -\frac{a}{2} \leq x < 0 \tag{1.12}$$

The composite panels were manufactured using a Viper 4000 Automated Fiber Placement machine. The panels were laid up on a flat steel tool which was sequentially vacuum-bagged for each ply. A vacuum was applied throughout the AFP process and maintained during deposition to ensure proper consolidation of the fiber courses. Each fiber course was formed by gathering eight tows, resulting in a nominal course width of 25.4 mm, with an individual tow width of 3.175 mm. The fiber paths were discretized into individual tows and deposited using the Viper 4000 control software, which automatically distributed the course placement based on the predefined reference fiber path. Potential manufacturing issues, such as wrinkles and fiber placed laminates, were identified by the software during the layup process. To enforce the prescribed variation of fiber angle, tow drops were introduced when necessary, resulting in either gaps or overlaps between adjacent courses. In this study, specific manufacturing strategies were adopted to ensure 100 percent gaps (complete gaps) and 100 percent overlaps (complete overlaps), allowing the isolated investigation of each defect type. Upon completion of the layup process, the panels were cured in an autoclave. Particular care was taken during shaping to maintain straight edges, along which the compressive load was applied during the experimental tests, thereby ensuring uniform load introduction and preventing premature failure.

Prior to the main experimental campaign, the panels were instrumented with eight paired axial strain gauges installed on opposite surfaces. To verify the suitability of the selected gauge locations and ensure the reliability of the strain measurements, three preliminary compression tests were performed under low load levels. This preliminary phase was essential, as the experimental responses were subsequently compared with the corresponding analytical predictions, enabling a consistent validation of the adopted modeling framework.

For all tested configurations, the experimental buckling response, exhibits an initial non linear region, followed by a linear pre-buckling regime and a progressively non linear post-buckling behavior. The initial non linearity is primarily attributed to unavoidable imperfections in the loading and boundary conditions rather than to intrinsic material effects. The pre-buckling stiffness was extracted from the slope of the linear portion of the load-displacement curves, while the critical buckling load was identified as the point at

which a clear deviation from linearity occurs. Although geometric imperfections prevent the identification of a sharp bifurcation point, this definition provides a consistent and repeatable criterion for comparing different panel configurations.

When compared to the baseline laminate, the variable stiffness panels demonstrate a clear sensitivity to the adopted manufacturing strategy. Panels manufactured with complete overlaps exhibit a significant increase in both axial stiffness and critical buckling load, whereas configurations dominated by gaps show a degradation of these quantities. The results indicate that the local thickness increase associated with overlaps enhances global stability, while resin rich regions generated by gaps reduce the load carrying capability of the structure, as shown in Table 1.4.

Table 1.4: Pre-buckling stiffness and critical buckling load obtained through experimental and numerical tests. Source: [18]

Panel configuration	K_0 (kN/mm)		P_{cr} (kN)	
	Experimental	Numerical	Experimental	Numerical
Quasi-isotropic panel	34.59	33.23	11.52	13.08
Panel with complete overlaps	47.18	46.46	20.80	21.14
Panel with complete gaps	33.68	32.52	12.32	13.52

The strain gauge measurements provide further insight into the deformation mechanisms governing the structural response, as it is shown in Figure 1.12. Within the pre-buckling regime, the strain readings from opposite faces are nearly identical, indicating a predominantly membrane dominated behavior and confirming the effectiveness of the load introduction. As the applied load increases and buckling is approached, a progressive divergence between the strain readings becomes evident, revealing the onset of bending deformation consistent with global instability. Moreover, strain measurements collected at symmetric locations with respect to the panel centerline exhibit similar trends, indicating that the overall deformation pattern remains symmetric despite the presence of manufacturing induced gaps and overlaps.

Overall, these observations indicate that defects induced by automated fiber placement predominantly influence the global stiffness and buckling resistance of variable stiffness panels rather than triggering localized asymmetric deformation modes. Consequently, the structural implications of gaps and overlaps can be effectively assessed through global performance metrics, supporting the use of homogenized modeling strategies for the numerical analysis of such laminates, provided that manufacturing effects are consistently accounted for. Despite their effectiveness at the analysis stage, the homogenized modeling

approaches adopted by Marouene et al. inherently evaluate manufacturing effects once the fiber architecture has already been defined. This limitation highlights the need for design frameworks in which manufacturing constraints are embedded directly within the definition and optimization of the fiber paths rather than treated as corrections of the model.

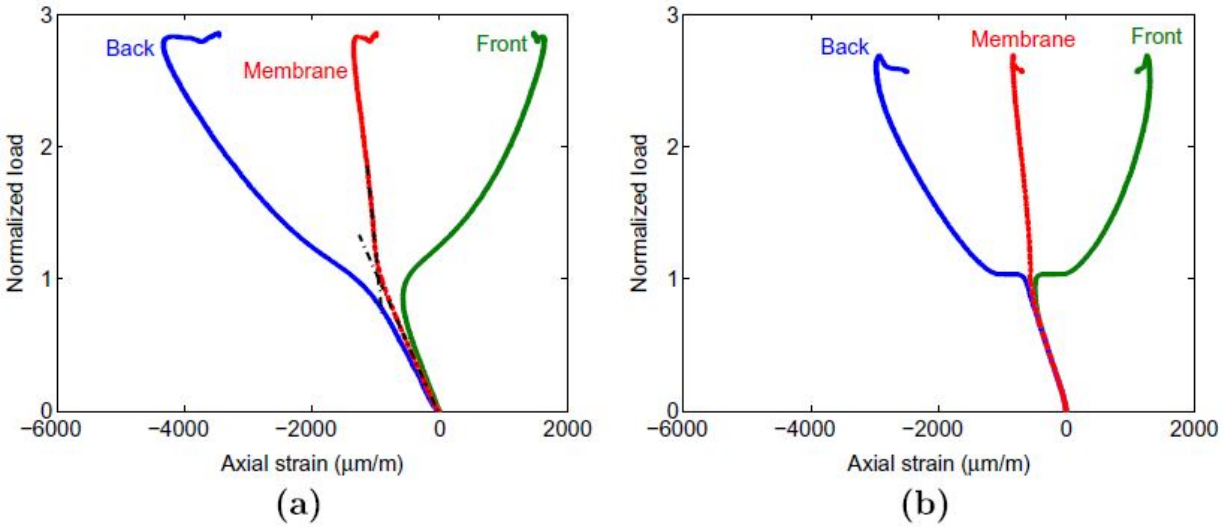

Figure 1.12: Normalized load vs strain gauges for (a) panels with complete overlaps (b) panels with complete gaps. Source: [18]

2 | Robotic Automatic Fiber Placement

Robotic Automated Fiber Placement (RAFP) represents a significant evolution of the Automated Fiber Placement (AFP) process. By enabling explicit control over course discretization, steering limitations, and thickness build ups, RAFP allows features arising from the manufacturing process to be deliberately incorporated into the design process. Building on the understanding established by Marouene et al. regarding the contrasting roles of overlaps and gaps, recent approaches based on RAFP demonstrate how thickness variations arising from manufacturing can be strategically leveraged to improve global stiffness and buckling performance. This transition from defect aware analysis to manufacturing aware design represents a key step toward the development of variable stiffness laminates that are both structurally efficient and practically realizable.

Robotic Automated Fiber Placement (RAFP) represents a significant evolution with respect to conventional AFP, not only in terms of hardware configuration, but more importantly in the way manufacturing constraints are integrated into the design process. While traditional AFP systems typically rely on portal frame architectures with limited flexibility in tool accessibility and course placement, RAFP employs multi axis robotic manipulators that enable enhanced control of the deposition process over complex geometries. This increased kinematic freedom allows for more precise control of tow steering, course spacing, and deposition sequence, but at the same time introduces a distinct manufacturing signature associated with robotic motion, discretization of fiber courses and machine dependent steering constraints.

From a design perspective, this shift fundamentally alters the role of manufacturing induced features such as gaps, overlaps, and local thickness variations. In conventional analyses based AFP, these features are often treated as unavoidable imperfections that are identified and assessed only after the fiber architecture has been defined. In contrast, the RAFP framework explicitly acknowledges that such features are an intrinsic consequence of robotic deposition and must therefore be considered during the design stage.

As a result, manufacturing constraints are no longer treated as secondary effects, but become governing parameters that directly influence the admissible fiber paths and the resulting structural performance. This paradigm shift enables a tighter coupling between fiber steering strategies, realistic manufacturability, and global performance objectives such as in-plane stiffness and buckling resistance.

In the proposed RAFP-based modeling framework [27], the fiber paths are not prescribed through analytical steering laws, but are instead constructed by interpolating a set of control points using Bézier curves. In particular, cubic Bézier splines are employed to define the centerlines of individual fiber courses. This choice is motivated by the fact that cubic Bézier curves represent the lowest-order polynomial formulation capable of introducing an inflection point along the fiber path, which is essential for accurately describing steering patterns required to tailor the structural response while maintaining manufacturability.

The use of cubic splines enables smooth and continuous variation of fiber orientation along the course length, while providing sufficient flexibility to capture complex curvilinear trajectories within the curvature limits imposed by the RAFP process. Higher order polynomial representations were not adopted as they would increase the number of control parameters without offering additional practical benefits in terms of steering capability. Conversely, lower order curves would be unable to reproduce the inflection behavior necessary for achieving the desired redistribution of stiffness and buckling resistance. As a result, cubic Bézier splines offer an effective compromise between geometric flexibility and modeling efficiency. The Bézier-based fiber path is described by the Cartesian parametric expressions reported in Equation (2.1) and Equation (2.2), where x_i and y_i $(i = 1, 2, 3, 4)$ denote the coordinates of the control points.

$$x(t) = x_1(1-t)^3 + 3x_2t(1-t)^2 + 3x_3t^2(1-t) + x_4t^3, \qquad 0 \leq t \leq 1 \tag{2.1}$$

$$y(t) = y_1(1-t)^3 + 3y_2t(1-t)^2 + 3y_3t^2(1-t) + y_4t^3, \qquad 0 \leq t \leq 1 \tag{2.2}$$

In addition to the use of cubic Bézier splines for defining the fiber course centerlines, the modeling framework introduces a dedicated interpolation scheme based on a so called manufacturing mesh. Rather than directly optimizing the coordinates of the Bézier control points, the approach defines a structured grid over the design domain, referred to as the manufacturing mesh, whose nodal locations serve as interpolation points for updating the fiber paths. This strategy significantly reduces the number of optimization variables, as

the control points of each spline are constrained to lie on a locus curve obtained through interpolation within the manufacturing mesh.

An initial configuration, denoted as the initial seed, is first defined by placing a set of straight fiber courses with no gaps or overlaps, ensuring full coverage of the panel. The Bézier control points associated with this initial seed are collinear and represent the undeformed reference configuration. During the optimization process, the nodal locations of the manufacturing mesh are then shifted by prescribed nodal shift distances, which constitute the primary design variables. These nodal shifts are interpolated to update the positions of the Bézier control points according to their original coordinates, thereby generating new fiber paths while preserving continuity and manufacturability. The interpolation scheme ensures that adjacent fiber courses do not intersect or cross each other, as all control points are constrained to follow the same locus curve within a given manufacturing mesh element. As a result, the relative spacing between neighboring courses remains controlled, allowing the extent of gaps and overlaps to be implicitly bounded within the design space, as it is shown in Figure 2.1. By decoupling the definition of the fiber paths from the direct manipulation of individual control points, this interpolation based methodology enables a systematic exploration of manufacturable designs while maintaining a clear link between the manufacturing parameters and the resulting fiber architecture.

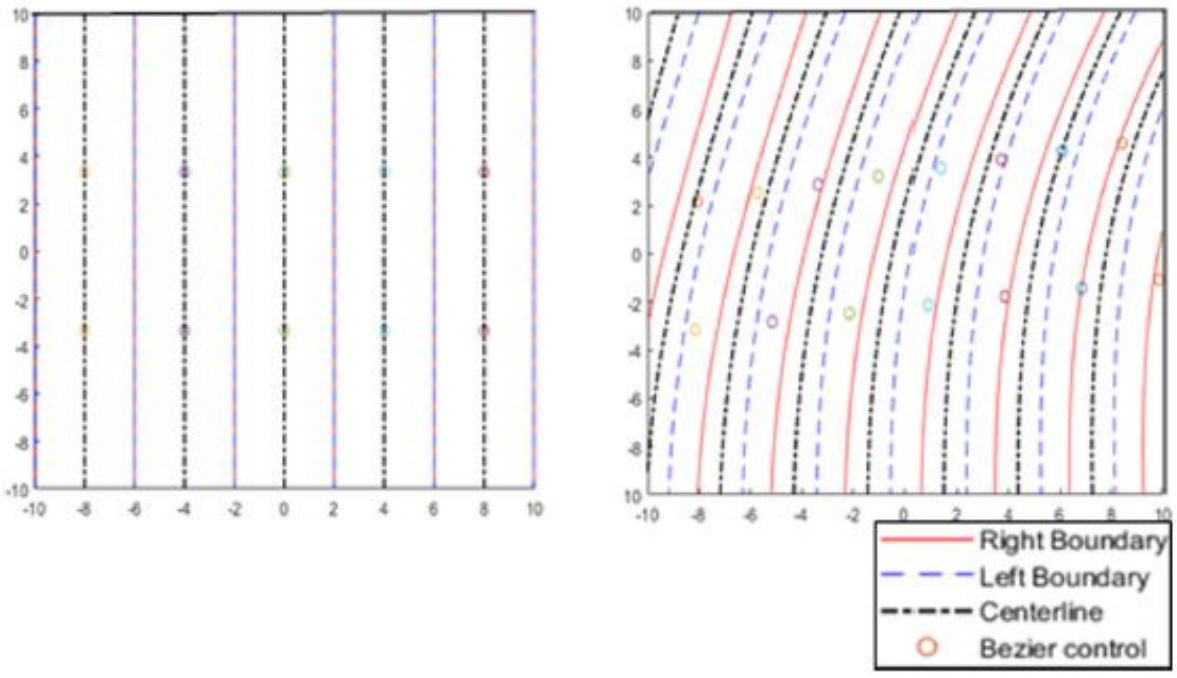

Figure 2.1: Varying steered fiber courses in a design. Source: [27]

The finite element models are constructed using a pixelated mesh approach, in which the panel surface is discretized into a structured grid of quadrilateral shell elements composed of 40,401 nodes, each characterized by three translational and three rotational degrees of freedom. This level of discretization is selected to ensure an adequate resolution of the spatial variation of fiber orientation and thickness induced by the RAFP process, while maintaining a manageable computational cost.

Unlike approaches in which the finite element mesh is aligned with the fiber courses, the pixelated mesh adopted here is independent of the manufacturing mesh used to define the fiber paths. For each finite element and for each ply within the laminate stack, the algorithm identifies the fiber courses that pass through the element centroid. The local fiber orientation is then assigned by determining the tangent direction of the corresponding Bézier-defined fiber path evaluated at the closest point to the element centroid. This procedure ensures a consistent mapping between the manufacturing-informed fiber architecture and the finite element representation, without requiring the structural mesh to conform to the course geometry.

The pixelated formulation further enables the identification of multiple fiber courses intersecting a single finite element. In such cases, the element is assigned a thickness corresponding to the combined contribution of all intersecting courses. When a single course is identified within an element, a nominal ply thickness consistent with the manufacturing parameters of the RAFP process is assigned. Conversely, if multiple courses overlap within the same element, each course is assigned 95 percent of the nominal ply thickness, in accordance with previous experimental observations indicating that overlap thickness does not scale linearly with the number of superposed tows. This assumption allows thickness build ups associated with overlaps to be incorporated into the model in a physically realistic manner.

By decoupling the structural mesh from the manufacturing mesh, the pixelated approach enables manufacturing induced features such as gaps, overlaps, and thickness variations to emerge naturally from the interaction between the discretized fiber architecture and the finite element model. As a result, the mechanical response of the laminate can be evaluated while explicitly accounting for effects induced by RAFP, without resorting to mesh refinement strategies or homogenization assumptions that could obscure the underlying manufacturing physics.

Traditional approaches based on AFP typically treated manufacturing induced imperfections as implicit or secondary features to be evaluated after the structural model had been constructed. In previous works such as [12], defects were incorporated into numeri-

cal models through homogenized variables representing defect area percentages, effectively capturing the influence of gaps and overlaps within a binary or continuous defect layer formulation, without explicitly linking the defect geometry to the underlying deposition kinematics. Similarly, the modeling strategies adopted in [18] relied on predefined fiber trajectories derived from analytical expressions and introduced gaps or overlaps through local modifications of the ply properties, thereby evaluating the effect of manufacturing imperfections primarily as perturbations superimposed on otherwise ideal fiber paths. In contrast, RAFP based frameworks represent a more integrated perspective in which the definition of fiber paths and the emergence of manufacturing induced features are directly coupled with the structural model. Rather than relying on pre specified analytical functions or defect layers, RAFP employs interpolation schemes combined with cubic Bézier splines to generate fiber course centerlines from a set of control points defined on a manufacturing mesh. This approach has two important consequences. First, the fiber paths are inherently manufacturable by construction, as they are generated within the curvature and steering limitations of robotic placement systems. Second, features such as course discretization, localized thickness build ups, and relative gaps or overlaps arise naturally from the interaction between the manufacturing mesh and the defined fiber paths, rather than being imposed through corrective adjustments after mesh generation. Moreover, whereas earlier approaches often required mesh refinement or extensive post processing to capture the local geometry of defects, the interpolation and pixelated mesh strategy adopted in the RAFP framework allows manufacturing induced variations to be represented implicitly through the mapping of fiber orientations and thickness within a structured finite element grid. This represents a fundamental methodological shift, as manufacturing constraints and defect signatures are embedded in the structural model from the outset, enabling a unified analysis of stiffness and buckling performance that directly reflects the geometric and kinematic characteristics of the deposition process.

The buckling results obtained from the numerical analyses indicate that the adoption of RAFP manufactured structures leads to a consistent enhancement of the critical buckling load under both uniaxial and biaxial loading conditions. These results are based on six distinct designs selected from an optimized set of feasible solutions, each characterized by a different fiber path configuration derived from a multi objective design process aimed at maximizing buckling resistance while minimizing structural mass. Despite the differences in fiber architecture among the selected designs, all configurations exhibit improved buckling performance with respect to the benchmark configuration, highlighting the robustness of the RAFP based approach.

In the uniaxial compression case, the tailored fiber paths and the associated thickness

variations generated through the RAFP process promote a more efficient redistribution of stiffness, delaying the onset of global instability. Similarly, under biaxial loading, the optimized fiber architectures exhibit improved load carrying capability, demonstrating increased resistance to buckling despite the presence of manufacturing induced features such as gaps, overlaps, and local thickness build ups. The results discussed are presented in Table 2.1.

Table 2.1: Normalized buckling loads for steered and baseline laminates under uniaxial and biaxial loading conditions. Source: [27]

Panel configuration	**Steered**	**Base**	**Increase**
Uniaxial loading			
Design 1	0.8129	0.5709	42%
Design 2	0.7820	0.5709	37%
Design 3	0.7768	0.5709	36%
Biaxial loading			
Design 1	0.2638	0.1940	36%
Design 2	0.2688	0.1940	37%
Design 3	0.2718	0.1940	41%

These improvements in buckling performance, observed across different loading scenarios, highlight the robustness of the RAFP based design framework. By explicitly integrating manufacturing constraints into the definition of the fiber paths, the resulting structures achieve superior stability characteristics without relying on idealized assumptions or corrective defect adjustments introduced after modeling. As a consequence, RAFP emerges as a particularly suitable manufacturing technology for lightweight and large scale aeronautical structures, where buckling resistance often represents a governing design criterion.

Despite the enhanced global stability demonstrated in the previous analyses, the structural performance of aeronautical components is frequently governed by localized phenomena rather than by global instability alone. In particular, stress concentrations arising around geometric discontinuities such as cutouts, stiffener terminations, or load introduction regions can dominate damage initiation mechanisms and ultimately limit the structural efficiency of composite structures.

Recognizing this limitation, in a subsequent study [30] the authors extend the same manufacturing aware RAFP framework to address the mitigation of stress concentrations. The focus of this work is to investigate how tailored fiber steering can be employed to reduce peak stresses in the vicinity of geometric discontinuities, while explicitly accounting for

the manufacturing signatures inherent to robotic fiber placement. Since the study is conducted by the same research group and builds directly upon the previous framework, the underlying modeling and parametrization strategies remain unchanged.

Specifically, in both studies the modeling of the steered fiber trajectories and their parametrization follow the same formulation. The fiber paths are described using cubic Bézier splines, which ensure geometric continuity of the fiber courses and allow manufacturing constraints such as minimum steering radius and course width to be directly incorporated into the design space. This formulation also guarantees complete coverage of the panel domain, even in the presence of complex geometries. As illustrated in Figure 2.2, two different manufacturing strategies can be adopted to realize panels with cutouts. In both cases, full coverage of the structure is ensured. However, in one approach the fiber courses are steered to follow the geometry of the cutout, whereas in the other the courses are deposited continuously and the cutout is subsequently introduced through material removal.

Previous studies ([1] [3]) have demonstrated that the former strategy is generally more advantageous from a structural standpoint. By allowing the tows to follow the geometry of the discontinuity, the fibers are better aligned with the local load paths, resulting in more efficient load transfer and consequently enhanced structural performance compared to configurations in which the cutout is introduced after deposition.

The parametrization of these trajectories remains unchanged and relies on the same interpolation scheme based on a dedicated manufacturing mesh. This mesh, defined independently from the structural finite element discretization, governs the spatial distribution of the Bézier control points through interpolation, thereby enforcing smooth and coherent variations of fiber orientation across the structure while limiting the number of independent design variables. In addition, manufacturing induced effects associated with the RAFP process, including gaps and overlaps between adjacent courses, are explicitly represented at the course level and incorporated into the structural description through spatial variations of the laminate properties.

The main distinction between the two studies lies in the formulation of the optimization problem. While the previous work adopts a multi objective optimization framework aimed at identifying trade offs among multiple structural performance metrics, with particular emphasis on global buckling behavior, the subsequent study focuses on a single design objective, namely the minimization of the Stress Concentration Factor (SCF). In this case, the optimization process is specifically directed toward reducing the SCF under the assumption that a more uniform stress distribution represents the dominant requirement for improving structural performance in the presence of geometric discontinuities.

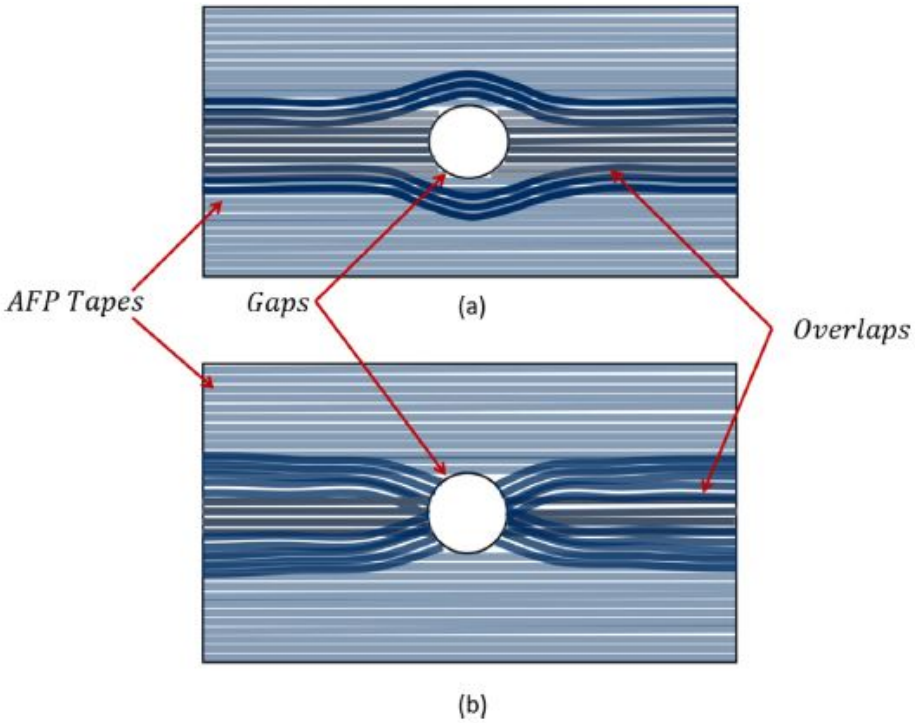

Figure 2.2: Courses laid up to create a cut out (a) Fiber path that goes around the cut out (b) Fuber path that end at/start at the cut out. Source: [30]

The structure investigated consists of one quarter of a flat panel containing a centrally located circular cutout. Owing to the geometric and loading symmetries of the problem, this reduced domain is sufficient to capture the complete structural response. The numerical results show a reduction of approximately 32 percent in the stress concentration factor with respect to the baseline configuration, represented by a quasi isotropic laminate. This improvement is achieved with a limited penalty in terms of mass and global stiffness. The optimized panel exhibits an increase in weight of approximately 3 percent compared to the baseline, while the axial stiffness along the global loading direction is reduced by only 3 percent.

A comparison of the stress distributions further highlights the benefits of the optimized fiber steering strategy. As shown in Figure 2.3, the optimal configuration exhibits a more uniform stress field around the cutout, with peak stresses distributed over a broader region rather than concentrated at a single location. In contrast to the quasi isotropic laminate, where the maximum stress is primarily localized at the inner edge of the cutout, the design with steered fibers promotes a smoother redistribution of stresses, thereby reducing the severity of local stress concentrations.

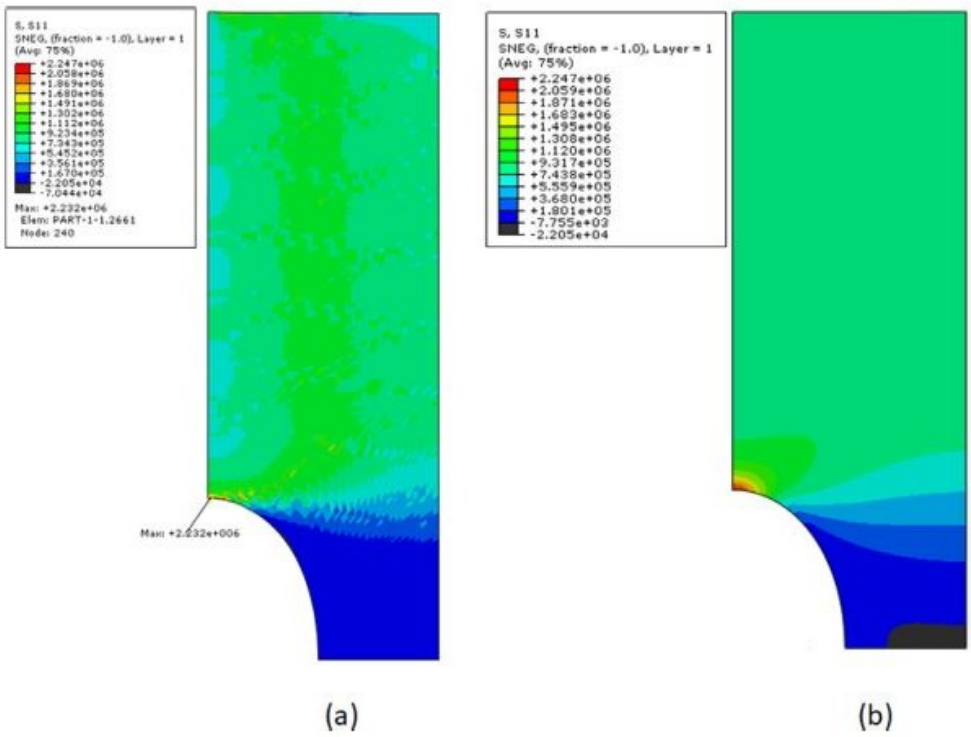

Figure 2.3: Contour of σ_{11} in (a) Optimal solution (b) Quasi-isotropic laminate. Source: [30]

3 | Implementation of defects in FEM pre-processing

Building upon the manufacturing aware frameworks discussed in the previous sections, the present work introduces a numerical model developed to characterize the local laminate architecture of composite panels with straight or steered fibers, including hybrid laminate configurations. Given a prescribed stacking sequence and the geometry of a rectangular panel with a centrally located cutout, the model determines the number of plies intersecting each nodal location. This information provides a local description of the laminate build up that is directly linked to the underlying fiber placement strategy.

The fiber paths are described using the analytical formulation originally proposed by Tatting, Equation (1.1), which enables a continuous and spatially varying representation of fiber orientations while remaining compatible with automated fiber placement constraints such as tow width. Based on this formulation, the model tracks the spatial distribution of individual plies across the panel domain and evaluates their intersection with the discretized nodal locations. As a result, the model identifies regions exhibiting local increases or decreases in material presence, corresponding to areas potentially dominated by overlaps or gaps induced by fiber steering.

The definition of the fiber paths does not explicitly account for the presence of the cutout. This choice is consistent with the approach adopted by Tatting in his studies. The fiber architecture is first defined over the full unperforated panel domain, and the cutout is subsequently introduced at the geometric level. This modeling choice reflects a common assumption in idealized design studies, in which the fiber layout is generated independently of local geometric discontinuities, allowing the effects of the cutout to be examined without modifying the underlying fiber path formulation.

The primary objective of this implementation is not to directly evaluate structural performance, but rather to establish a geometric description of the laminate that can serve as a foundation for subsequent analyses. By explicitly quantifying the number of plies contributing at each nodal location, the model provides a systematic means of correlating

prescribed fiber paths with local variations in laminate architecture, independently of any specific structural response metric.

The numerical model was implemented in MATLAB and generates a discretized representation of the panel domain based on the prescribed geometry. The panel is discretized using triangular elements, which allow accurate representation of the geometric discontinuity. The mesh density is selected to be sufficiently fine to capture local variations in laminate thickness while avoiding excessive computational cost. Once the mesh is defined, the fiber placement process is simulated beginning with the generation of a reference tow which is obtained from the analytical formulation introduced previously by evaluating the fiber orientation angle $\theta(r)$ at a set of predefined control points. These points are then interpolated using a spline method to reconstruct a continuous representation of the tow path across the panel domain. The reference tow is subsequently replicated by offsetting it in the direction normal to the course until full coverage of the panel surface is achieved.

At this stage, a geometric intersection procedure is employed to determine which mesh nodes are intersected by each tow. Each course is assumed to have constant thickness corresponding to a single ply and constant width equal to 0.3175 cm. By identifying the nodes lying within the tow width, the local ply thickness contribution is assigned at the nodal level. This procedure is repeated for all plies defined in the stacking sequence, ultimately resulting in a nodal representation of the laminate thickness distribution over the entire panel.

The numerical model is illustrated by considering a rectangular composite panel with dimensions 37.1 cm$\times$50.7 cm, featuring a centrally located circular cutout of 7.62 cm. The laminate stacking sequence adopted in this case is $[\pm 45/0/\pm 45/60_2/0/\pm 30/15/\pm 45/60]_s$. Figure 3.1 shows the resulting nodal distribution of laminate thickness obtained from the proposed modeling framework.

The predicted thickness distribution is consistent with the geometric thickness variation hypothesized by Tatting for a laminate with these characteristics, reflecting the underlying fiber placement strategy and the associated material accumulation patterns. In particular, regions of increased and reduced thickness follow the same qualitative trends expected from the idealized geometric description.

Minor discrepancies between the present results and the idealized thickness distribution are observed and can be attributed to the discretized nature of the proposed model. Since the laminate architecture is evaluated on a finite mesh and the fiber paths are represented through discrete tow replication, an exact match with the continuous geometric formulation is not expected. Nevertheless, the overall agreement between the two distributions

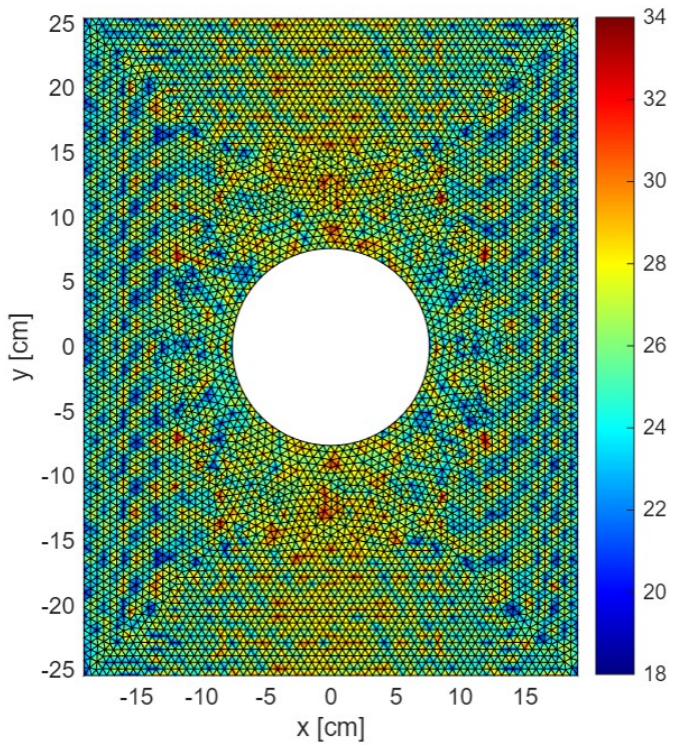

Figure 3.1: Number of tows intersecting each mesh node in the perforated panel.

confirms that the model captures the essential features of the thickness variation induced by fiber steering, thereby providing a consistent validation of the proposed approach.

Beyond its illustrative purpose, the proposed modeling framework provides a basis for future investigations aimed at assessing the structural implications of manufacturing induced thickness build ups in steered fiber composite panels. By delivering a detailed nodal description of the local laminate architecture, the model establishes a direct link between fiber placement strategies and spatial variations in laminate thickness. This information can be exploited in subsequent analyses to evaluate how local thickness variations influence both global and local structural performance metrics, such as the critical buckling load or the in plane and bending stiffness of the panel. From this perspective, the present model represents a preliminary yet essential step toward the integration of manufacturing aware laminate descriptions into structural analyses. It enables the systematic incorporation of gaps, overlaps, and localized material accumulation into design methodologies focused on structural performance.

4 | Conclusion

This thesis has examined the behavior of variable stiffness composite laminates by progressively moving from idealized stiffness tailoring concepts toward laminate descriptions compatible with realistic fiber placement processes. Starting from the limitations of classical laminates with straight fibers, the evolution toward curvilinear and steered fiber architectures has been reviewed, showing how fiber steering enables a more effective alignment between material stiffness and spatially varying load paths. Early physically motivated approaches highlighted the potential of this concept, while subsequent optimization based formulations provided systematic tools for improving structural performance, particularly with respect to buckling behavior.

The literature analysis has shown that the translation of continuous fiber orientation fields into realizable laminates is inevitably accompanied by geometric features such as gaps and overlaps. In many idealized modeling approaches, these features are naturally accounted for as a direct consequence of the discrete nature of the material system and of the assumptions adopted to represent fiber courses and laminate architecture. Within this context, numerous numerical and experimental investigations have demonstrated that such features can influence the global stiffness and stability of composite panels, motivating continued efforts to describe their effects with greater geometric fidelity.

Within the same framework, Robotic Automated Fiber Placement represents a significant technological development, as it enables enhanced control over fiber steering, course discretization, and laminate build up. Consequently, geometric features such as gaps and overlaps are no longer solely the result of manufacturing execution, but can be anticipated and regulated during the definition of the fiber paths. Compared to conventional automated placement techniques, RAFP allows fiber trajectories and laminate geometry to be prescribed in closer correspondence with the actual deposition process, enabling a more deliberate control of the resulting laminate architecture.

On the basis of these considerations, the present work has introduced a numerical model aimed at describing the local laminate architecture associated with steered fiber placement. The model provides a geometric and topological representation of the laminate

by mapping the spatial distribution of laminate thickness resulting from prescribed fiber paths. The resulting thickness distributions are consistent with theoretical geometric expectations while naturally reflecting the discretized nature of the fiber placement process. Although the current formulation is limited to a geometric description of the laminate, it establishes a suitable foundation for subsequent structural analyses. In particular, the model can be coupled with numerical methods to investigate how local thickness variations influence structural quantities such as panel stiffness and critical buckling load. In this sense, the work contributes to establishing a more direct connection between fiber placement strategies and structural assessment, supporting the analysis of variable stiffness composite panels with increasing geometric realism.

Bibliography

[1] M. W. Hyer and R. F. Charette, "Innovative design of composite structures: The use of curvilinear fiber format in composite structure design," NASA, Virginia Polytechnic Institute and State University, Tech. Rep. VPI-E-90-04, 1990.

[2] M. W. Hyer, "Stress analysis of fiber-reinforced composite laminates with curvilinear fiber paths," *AIAA Journal*, vol. 29, no. 6, pp. 1011–1015, 1991.

[3] M. W. Tosh and D. W. Kelly, "On the design, manufacture and testing of trajectorial fibre steering for carbon fibre composite laminates," *Composite Structures*, 2000.

[4] B. F. Tatting and Z. Gürdal, "Design and manufacture of elastically tailored tow placed plates," NASA Langley Research Center, Tech. Rep. NASA/CR-2002-211919, 2002.

[5] Z. Gürdal, B. F. Tatting, and C. K. Wu, "Variable stiffness composite panels: Effects of stiffness variation on the in-plane and buckling response," *Composites Part A: Applied Science and Manufacturing*, vol. 39, pp. 911–922, 2008.

[6] S. Setoodeh, M. M. Abdalla, S. T. Ijsselmuiden, and Z. Gürdal, "Design of variable-stiffness composite panels for maximum buckling load," *Composite Structures*, 2008.

[7] A. W. Blom, C. S. Lopes, P. J. Kromwijk, Z. Gürdal, and P. P. Camanho, "A theoretical model to study the influence of tow-drop areas on the stiffness and strength of variable stiffness laminates," *Computational Materials Science*, vol. 43, pp. 403–425, 2009.

[8] A. W. Blom, "Buckling and post-buckling of variable stiffness composite cylinders," PhD thesis, Delft University of Technology, 2010.

[9] C. S. Lopes, Z. Gürdal, and P. P. Camanho, "Tailoring for strength of composite steered-fibre panels with cutouts," *Composite Structures*, 2010.

[10] A. J. M. Ferreira, E. Carrera, and M. Cinefra, "Buckling analysis of variable stiffness composite plates," *Composite Structures*, vol. 93, pp. 2424–2434, 2011.

[11] Z. Wu, G. Raju, and P. M. Weaver, "Buckling analysis and optimisation of variable angle tow composite plates," *Thin-Walled Structures*, vol. 60, pp. 163–172, 2012.

[12] K. Fayazbakhsh, M. A. Nik, D. Pasini, and L. Lessard, "Defect layer method for the analysis of variable stiffness composite laminates with gaps and overlaps," *Composite Structures*, vol. 97, pp. 145–158, 2013.

[13] B. H. Coburn, Z. Wu, and P. M. Weaver, "Buckling analysis of stiffened variable angle tow panels," *Composite Structures*, vol. 111, pp. 259–270, 2014.

[14] B. C. Kim and K. Potter, "Manufacturing considerations for tow-steered composite laminates," *Composites Part A: Applied Science and Manufacturing*, vol. 61, pp. 200–212, 2014.

[15] Z. Wu, P. M. Weaver, and G. Raju, "Postbuckling optimization of variable angle tow composite plates," *Composite Structures*, vol. 111, pp. 259–270, 2014.

[16] D. Baraccani, "Analisi del comportamento a fatica di un laminato al variare della sequenza di impilamento e delle dimensioni," Tesi di Laurea Magistrale, Alma Mater Studiorum – Università di Bologna, Bologna, 2015.

[17] Y. Li, "Modelling the effect of gaps and overlaps in automated fibre placement (afp) manufactured laminates," *Science and Engineering of Composite Materials*, 2015.

[18] A. Marouene, R. Boukhili, J. Chen, and A. Youssefpour, "Effects of gaps and overlaps on the buckling behavior of an optimally designed variable-stiffness composite laminates – a numerical and experimental study," *Composite Structures*, vol. 146, pp. 17–25, 2016.

[19] R. Vescovini and L. Dozio, "A variable-kinematic model for variable stiffness plates: Vibration and buckling analysis," *Composite Structures*, vol. 142, pp. 15–26, 2016.

[20] T. R. Brooks and J. R. R. A. Martins, "On manufacturing constraints for tow-steered composite design optimization," *Composite Structures*, vol. 204, pp. 548–559, 2018.

[21] R. Vescovini and L. Dozio, "Thermal buckling behaviour of thin and thick variable-stiffness panels," *Journal of Composites Science*, vol. 2, no. 4, pp. 1–23, 2018.

[22] Z. Wu, G. Raju, and P. M. Weaver, "Optimization of postbuckling behaviour of variable thickness composite panels with variable angle tows: Towards "buckling-free" design concept," *International Journal of Solids and Structures*, vol. 132–133, pp. 66–79, 2018.

[23] R. Vescovini, E. Spigarolo, E. Jansen, and L. Dozio, "Efficient post-buckling analysis of variable-stiffness plates using a perturbation approach," *Thin-Walled Structures*, vol. 143, pp. 1–12, 2019.

[24] A. Hyde, J. He, X. Cui, J. Lua, and L. Liu, "Effect of microvoids on strength of unidirectional fiber-reinforced composite materials," *Composites Part B*, 2020.

[25] R. Vescovini, V. Oliveri, D. Pizzi, L. Dozio, and P. M. Weaver, "A semi-analytical approach for the analysis of variable-stiffness panels with curvilinear stiffeners," *International Journal of Solids and Structures*, vol. 188-189, pp. 244–260, 2020.

[26] R. Vescovini, V. Oliveri, D. Pizzi, L. Dozio, and P. M. Weaver, "Pre-buckling and buckling analysis of variable-stiffness, curvilinearly stiffened panels," *Aerotecnica Missili & Spazio*, vol. 188-189, pp. 43–52, 2020.

[27] A. A. Vijayachandran and A. M. Waas, "Optimal fiber paths for robotically manufactured composite structural panels," *Composite Structures*, 2020.

[28] D. Cartié, M. Lan, P. Davies, and C. Baley, "Influence of embedded gap and overlap fiber placement defects on interlaminar properties of high performance composites," *Materials*, vol. 14, no. 18, p. 5332, 2021.

[29] E. Oromiehie, "Manufacturing defects in tow-steered composites," *Composite Structures*, 2021.

[30] A. A. Vijayachandran and A. M. Waas, "Minimizing stress concentrations using steered fiber paths and incorporating realistic manufacturing signatures," *International Journal of Non-Linear Mechanics*, vol. 146, p. 104 160, 2022.

[31] R. Vescovini, "Ritz r-function method for the analysis of variable stiffness plates," *AIAA Journal*, vol. 61, no. 6, pp. 2689–2701, 2023.

[32] A. Pagani, A. Racionero Sánchez-Majano, D. Zamani, M. Petrolo, and E. Carrera, "Fundamental frequency layer-wise optimization of tow-steered composites considering gaps and overlaps," *Aerotecnica Missili & Spazio*, 2024.

[33] P. Xiao, L. Bin, R. Vescovini, and S. Zheng, "Optimal design of composite sandwich panel with auxetic reentrant honeycomb using asymptotic equivalent model and pso algorithm," *Composite Structures*, vol. 328, p. 117 761, 2024.

[34] R. Vescovini, "The r-functions combined with the ritz method: An assessment on the integration schemes," *Composite Structures*, vol. 362, p. 119 066, 2025.

[35] R. Vescovini and P. P. Foligno, "Geometrically nonlinear analysis of variable-stiffness plates using the r-functions combined with the ritz method," *Acta Mechanica*, 2025.

[36] C. A. Yan and R. Vescovini, "A model reduction procedure based on the ps-fem for postbuckling analysis of composite shells," *Computers & Structures*, vol. 317, p. 107 907, 2025.

[37] C. A. Yan and R. Vescovini, "High-fidelity reduced-order method for postbuckling analysis of aeronautical structures," *AIAA Journal*, 2026.